Prediction of Removal of Ionic Solute during Electrodialytic Process and a Case Study

a thesis submitted
in partial fulfillment of the
requirements for the degree of

Master of Technology

by

Anurag Gupta

Department of Chemical Engineering

Indian Institute of Technology, Kanpur

February, 2002

CERTIFICATE

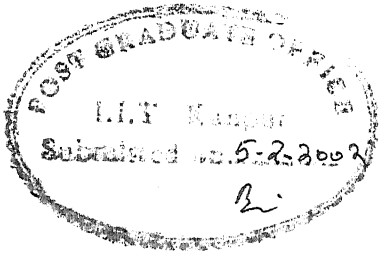

This is to certify that the work contained in this thesis, entitled **"Prediction of Removal of Ionic Solute during Electrodialytic Process and A Case Study"**, has been carried out by **Anurag Gupta** under my supervision and that this work has not been submitted elsewhere for a degree.

P. K. Bhattacharya

Dr. P. K. Bhattacharya
Department of Chemical Engineering
Indian Institute of Technology
Kanpur

5th February, 2002

Abstract

A theoretical approach was taken to analyze the process of electrodialysis (ED) and obtained results that may help to design the process. For the purpose, a boundary layer problem for ED with ion-exchange membranes was formulated and obtained results were analytically examined. Results are depicted for brine as feed in the middle compartment with a configuration of cation exchange membrane (CEM) and anion exchange membrane (AEM) in the right and left side of the compartment, respectively. Further, a mathematical model was developed with an objective to estimate the current density distribution as well as to obtain concentration profiles in diluate and concentrate channels as a function of width and length of channel. In diluate compartment, there was less depletion at the inward surface of the AEM whereas, there was much higher depletion at the inward surface of the CEM. As the channel length increased there was exponential decrease in the current density. Further, with increasing channel length average concentration was reducing, particularly during lower feed flow rates. Finally, a case study was conducted where earlier experimental results were utilized and fractional removal of calcium ion in presence of aqueous sucrose solution were analyzed. The developed model was accordingly modified by introducing an efficiency factor. The model prediction and experimental results were in agreement with little deviation. The deviations were attributed to the fouling surface of the membrane, which were not incorporated in the model.

ACKNOWLEDGEMENT

I express my deep sense of gratitude, respectful regards and sincere thanks to my thesis supervisor Dr. P. K. Bhattacharya for his discerning guidance, constructive advice and constant encouragement throughout the course of thesis work.

I also take the opportunity to express my thanks to all my friends for their inspiration and constant co-operation.

Finally, I would like to express my heartfelt appreciation to my family members for their love and support throughout the years. Their blessings have always shown me the right path in the most enduring moments of my life.

Anurag Gupta

Contents

LIST OF FIGURES

Nomenclature

c	Salt concentration (mol/l)
C	Dimensionless concentration (c/c_0)
d	Membrane thickness (m)
D	Diffusion coefficient ($m^2\ s^{-1}$)
f_R	Fractional removal
F	Faraday Constant
H	Channel width (m)
i	Current density ($A\ m^{-2}$)
I	Dimensionless current density (iH/FDc_0)
J_k	Flux of k-ions ($mol\ m^{-2}\ s^{-1}$)
Q	Volumetric flow rate (ml/min)
R	Universal gas constant
T	Solution Temp (K)
T_i	Transport number of i-ions in the solution
$\bar{T}_i$	Transport number of i-ions in the membrane
u_k	Mobility of ion-k ($m\ s^{-1}\ /(V\ m^{-1})$)
v	Velocity ($m\ s^{-1}$)
V	Dimensionless velocity ($v/\bar{v}$)
x,y	Coordinates (m)

X, Y	Dimensionless coordinates, $(x/H,\ yD/\bar{v}H^2)$
z_i	Charge number on i-ions
κ	Conductivity of the membranes $(\Omega^{-1}m^{-1})$
$\Delta\phi$	Electric potential drop (V)
Φ	Dimension less electric potential $(\phi F/(RT))$

Subscripts

0	Value at the channel inlet
ma	Anion exchange membrane
mc	Cation exchange membrane

Abbreviations

AA	Acetic acid
AEM	Anion exchange membrane
CEM	Cation exchange membrane
ED	Electrodialysis
EDTA	Ethylene diamine tetra acetic acid (di-sodium salt)

Chapter 1

Introduction

Electrodialysis (ED) is an electromembrane process in which ions are transported through ion selective membranes from one solution to another under the influence of an electrical potential gradient. The electrical charges on the ions allow them to be driven through the membranes fabricated from ion exchange polymers while applying a voltage between two end electrodes generates the potential field required for the purpose. Since the membranes used in ED have the ability to selectively transport counter-ions and reject co-ions, useful concentration, removal, or separation of electrolytes can be achieved by the process.

A common form of ED stack is shown in Fig 1.1, in which cation exchange membranes (CEM) and anion exchange membranes (AEM) are arranged alternately with electrodes on each end. When electric field is applied, due to selectivity of membranes a concentrated layer (salt rich) is produced on one side of membrane and a diluate layer (salt poor) on the other side. As a result of this demineralized product and concentrate streams are obtained in the alternate compartments. The diagram described in Fig 1.1 corresponds to one of the most common forms of the ED used for desalination and deionization purposes. There are, however several other types of ED processes. Donnan dialysis, diffusion dialysis, and isoelectrodialytic processes are closely related to conventional ED with various arrangements of ion exchange or neutral membranes and with or without an electrical potential driving force.

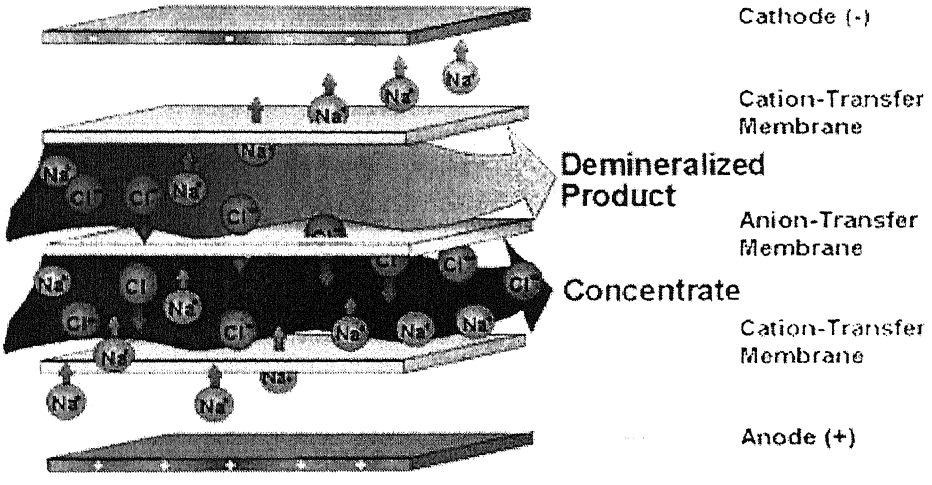

Fig 1.1 Electrodialysis Cell Pair

The large-scale application of ED is the production of potable water from brackish water. Here, the process competes with the processes of reverse osmosis and multistage flash evaporation. For water with relatively low salt concentration (less than 5000 ppm), ED is considered to be the most economic process [2]. Other main applications of ED include wastewater treatment, demineralization of cheese whey, concentrating acids and producing caustic and acid solutions with the aid of bipolar membranes. Further, nitrate removal from drinking water, desalting food products, tartaric wine stabilization, acid removal from organic product, conversion of organic salts into acid and base (bipolar membrane ED), desalting of amines, de-acidification of fruit juices, metals removal from ethylene glycol, edible salt production from seawater, desalting of surfactants, regeneration of electroless nickel plating baths, desalting of hydrolyzed vegetable proteins (i.e. soy sauce), concentration of dilute salt, acid, or base streams, recovery of salts, acids, and alkali from industrial rinse waters are also considered to be potential areas of application of ED.

Improvements in both the structure of ion-exchange membranes and the design of ED stacks have allowed ED to be considered as one of the technologies that can be introduced in various industries. One such industry, which may find the use of ED, is cane sugar processing industry, particularly for the removal of calcium ion from the processed juice, before crystallization operation. The sugar industry thus has to partially replace ion exchange resins for the demineralization and purification of sugar syrups. Conventionally, for the clarification and successive concentration of sugar juice, to obtain the pure crystallized sugar, there are two main objectives as per following:

- Removal of impurities:

  a) To separate insoluble solid matters suspended in juice in colloidal state rendering the juice opaque, viscous and dark in colour.

  b) To precipitate dissolved inorganic non-sugars.

- Bleaching effects:

  After impurities are removed by chemical treatment of the juice, bleaching is carried out to make the juice light colour for the manufacturing of white sugar.

The clarifying agents that are used for treatment of juice are lime, phosphoric acid, sulphur dioxide and carbon dioxide. Addition of lime, during the clarification stage introduces metal ions, mainly Ca^{++} in the clarified cane juice. Disadvantages caused by the presence of excess calcium or other alkaline earth metal ions and some heavy metal ions like iron, aluminum, etc. are:

a) Scale formation in the evaporators.

b) Improper crystallization.

c) Storage is hampered due to hygroscopic nature of these metals.

d) Excess calcium is unhygienic.

However, clarification of the juice is necessary as the extent of this treatment determines the purity and quality of the product (sugar). Keeping all shortcomings in the mind, these alkaline earth metals should be removed effectively before their entry into the evaporators. Membrane processes have the necessary ability to overcome many of these disadvantages of the conventional sugar process [19]. ED is one such potential process, which may address the problem of presence of calcium ion in the juice.

Increasing importance of ED has created the need to understand the process comprehensively. Through modeling and simulations the significance of physical parameters can be identified and process conditions can be optimized in a short time. Besides, the understanding of physico-chemical processes is improved. Nonetheless, experimental results are required to evaluate the developed model as well as to measure the model parameters.

In the present work, an attempt has been made to describe the problem of electrodialytic separation through a theoretical way, using a single monovalent electrolyte (NaCl) as solute. The work is presented in terms of theoretical modeling of a common ED stack. The objectives of the work are as follows:

- to predict concentration profiles in concentrate and diluate chamber.
- to predict rate of removal of solute.
- to study the influence other significant parameters on the rate of removal of solute.

Further, in order to evaluate the developed model experimental results abtained by Chattopadhyay [5] were taken as case study. The importance of the experimental investigations have been already discussed for removal of Ca^{++} ions through ED. Further, the experimental results were obtained using varying amount of Ca^{++}, for designed experimental purpose. Required details of the work have been provided in appendix 'A'.

Chapter 2

Literature Review

2.1 Fundamentals of Electrodialysis Operation

ED may be classified along with solvent extraction and reverse osmosis as a "selective transport" process. In these processes salt or solvent is transported away from the solution through a physical barrier without changing the state of any component in the system. In ED, separation is induced by an electric potential. As shown in Fig 2.1, this separation is accomplished by placing one or more sheets of material in which the transport numbers of ion differ from the values that prevail in the bulk solution on either side of the sheet across the path of the current.

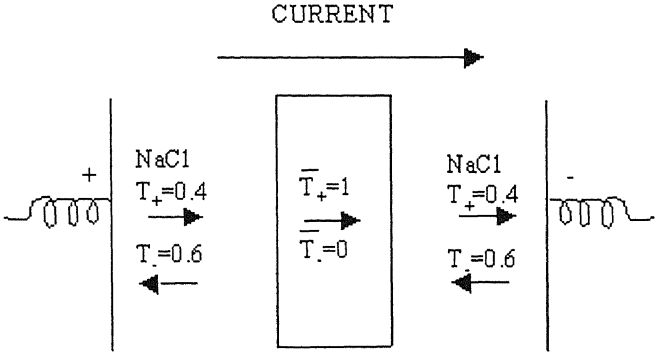

Fig 2.1: *Ion transport across a permselective membrane*

All the ED processes depend on the existence of a selective ion permeable membrane placed in the salt solution such a manner that a current flowing in the

solution must pass through the membrane. Passage of the electric current through the system will cause the formation of more concentrated layer on one side of the membrane and diluted layer on the opposite side. Of course diffusion tends to eliminate the concentration gradients that are induced by the flow of electricity, but the net result of the flow of electricity remains more or less unaffected.

2.2 Electroneutrality Condition

The movements of ion depends on its transport number (i.e. the fraction of the total current carried by a particular ion in the solution). To maintain the electroneutrality condition, an equivalent amount of the oppositely charged species should also move in the opposite direction and should be removed from the particular chamber. The relationship $T_+ + T_- = 1\left(\overline{T}_+ + \overline{T}_- = 1\right)$ guarantees that electroneutrality will be preserved [1].

2.3 Cation –Anion Exchange Membranes

The technical feasibility of ED as a mass separation process i.e. its capability of separating certain ions from a given mixture with other molecules, is mainly determined by the ion-exchange membranes used in the system. The principal requirements for a membrane to be useful in the ED process are:

- it must discriminate between ions of opposite charges.
- it must conduct electricity and must have low electrical resistance.
- its ion selectivity and permeability must be high.
- it should have high form-stability and good mechanical strength.
- it must also have low transference number for water.

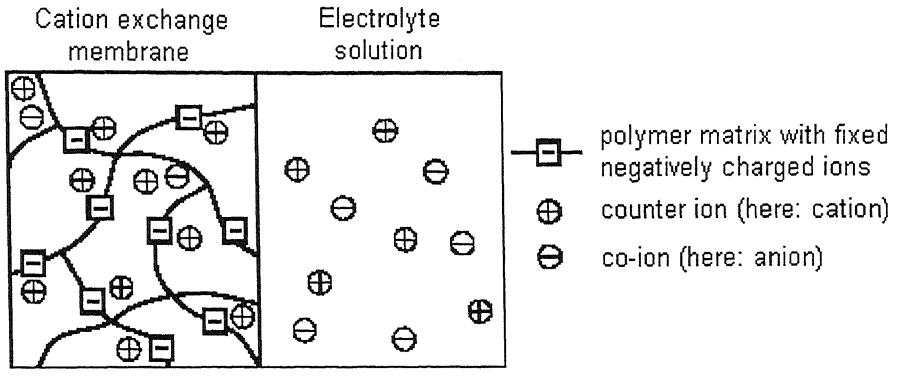

Fig 2.2:*Microscopic view of a Cation Exchange Membrane (CEM)*

Ion-exchange membranes are mostly ion exchange resins in differently prepared film form. These consist, therefore, of highly swollen gels carrying fixed positive or negative charges. Cation exchange membranes contain negatively charged groups fixed to the polymer matrix and anion exchange membranes contain positively charged groups fixed to the polymer matrix. The fixed ions in the matrix are in equilibrium with mobile ions (counter-ions). The ions (co-ions), which have identical charge as fixed charge, are more or less excluded from the polymer matrix due to equilibrium. This type of exclusion is called Donnan-exclusion [1,2].

The exclusion of the co-ions from the membrane phase leads, furthermore, to a build up of an electrical potential difference between the membrane and the adjacent dilute solution. This potential difference is called Donnan-potential [2].

2.4 Concentration Polarization and Limiting Current Density

In ED, it is desirable to operate at the highest practicable current density in order to get the maximum ion flux per unit membrane area. Operating current levels are, however, restricted by concentration polarization. This polarization results from

the difference in the transport numbers in the solution, where cations and anions carry roughly equal amounts of current, and in the highly selective ion exchange membrane, where virtually all the current is carried by the counter ions. The difference in transport number leads to a situation in which the solution close to the membrane surface on the diluate side becomes depleted of salt ions (fig2.3). At the same time the concentration near the membrane on the concentrate side increases [3]. This difference in ion concentration from bulk to membrane surface is termed as concentration polarization; where in an extreme condition, the diluate side boundary layer concentration may attain almost a negligible concentration. It is the most important phenomena, which is to be taken in to account any membrane process.

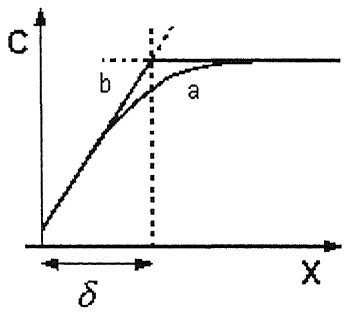

Fig 2.3: *Schematic of the real (a) and the idealized (b) concentration profile near the membrane - solution interface, δ is the diffusion boundary layer thickness.*

Due to this concentration variation across the membrane, diffusion plays an important role and the ion transfer rate is actually an added effect of diffusion and ionic mobility. Under unfavourable conditions, concentration may decrease to such a low value that no mineral ions are available for current transport any longer and then water dissociation starts [4]. This is indicated by any of the following:

- a drop in diluate pH level, leading to precipitation.
- an increase in electrical resistance leading to higher power consumption heat dissipation and water splitting.
- a transport of H^+ and OH^- ions, causing ED stack design problem.

Current density attained at this condition (diluate side reaching the value of negligible concentration) is called limiting current density [6]. On further raising the applied voltage, there is no significant increase in the cell current and therefore, limiting current density denotes the upper limit of the current through the stack.

Using Nernst [3] film model, limiting current density can be estimated as:

$$I_{\lim} = \frac{FC^{o}D}{\delta(T_m - T_s)} \tag{2.1}$$

where, δ, is diffusion boundary layer thickness, F is Faraday constant, D is diffusion coefficient, C^{o} is concentration in bulk and T_m, T_s are membrane and solution transport numbers, respectively.

2.5 Mass Transfer during Electrodialysis

In ED, the event of primary interest is the motion of ions under the influence of an electric field. Shaffer and Mintz [1] expressed the flux of ions in an electric field as:

$$J_k = u_k c_k (-\nabla\phi)\frac{z_k}{n_k} \tag{2.2}$$

where, J_k is flux of ion, u_k is electrical mobility of ion, c_k is the concentration of the ion, $\nabla\phi$ is the gradient of electric potential, z_k is the valance of the ion including algebraic sign and n_k is the number of equivalents in one mole.

If the ions pass through a region in which either u_k or c_k or both become very small, then clearly $J_k \simeq 0$. This fact provides ion-exchange membranes their selective characteristics.

The motion of the ion through a membrane is accompanied by a flow of electric current, and there may also be a flow of heat and a flow of solvent. Measurements by Shaffer and Ikeda [1] indicate that thermal gradients have a very minor effect on the flow of matter.

2.6 Fouling and Electrodialysis Reversal (EDR)

One of the problems in ED processes is that membranes and other active surfaces tend to become "fouled" or "scaled" over time by organic and inorganic substances present in the feed solution. The EDR process was developed and introduced in the early 1970's to deal with this problem. By reversing the electrical current and exchanging the feed and the product streams within the membrane stack several times per hour, fouling and scaling constituents that build up on the membrane surface in one cycle are removed in the next reversing cycle [2].

2.7 Removal of Ionic Species from Various Feed streams Using ED

The ED process should be operated below the limiting current density [11]. Cowon and Brown [12] studied the effect of turbulence on limiting current density in ED shells. They observed that although polarization can be destroyed by turbulent flow, however, polarization is more noticeable above a critical current density.

Tanaka [11] studied concentration polarization in the ED and observed that in the desalting chamber, if the convective flow rate (the flow rate component

perpendicular to the membrane surface) on the desalting surface of the membrane exceeds a critical value, the salt concentration distribution in the boundary layer becomes uniform and takes on the value for the bulk solution. However, if the convective flow rate drops even slightly below the critical value, the salt concentration in the boundary layer decreases considerably at the membrane solution interface.

Krol et al. [6,8] studied concentration polarization and observed that water dissociation is more pronounced in case of the anion exchange membrane than with the cation exchange membranes when applied current exceeds the limiting current density.

Bobreshova et al. [8] analyzed the voltage-current characteristics (VCC) of ED systems. They distinguished two sections according to the density of polarizing current, namely the under-limiting section and the over-limiting one. As far as the mechanism of ion transport in an over-limiting regime is concerned, there exist differences of opinions concerning participation of dissociated water ("water splitting") in the current transfer. The non-equilibrium phenomenon at the surface of the membrane on the side of the high salt concentration was said to take place at current densities much greater than the limiting value. It was shown that formation of a region of volume charge near the membrane might lead to passage of currents greater than the limiting current.

Wen et al. [10] reported that in the polarization of ED, the real ohmic resistance increase of the apparatus is not significant, whereas the main mechanism is a large fall in the net electrical motive force.

Tanaka et al. [7] studied distribution of electrodialytic condition in an electrodialyzer. When electrolyte solution is fed into the desalting cells in an

electrodialyzer and an electric current is passed across the membranes, the velocity or the electrolyte concentration of the solutions and electric current density usually change from place to place in the electrodialyzer.

Shaposhnik et al. [9] studied the dependence of the amino acid fluxes through the ion-exchange membranes during ED on the current density and found that this dependence is maximum at limiting current density. The decrease in amino acid fluxes explains the barrier effect of the polarized boundary layer near the membranes in the solution of the desalting compartment.

Huang et al [13] studied the effects of the Reynolds number, Schmidt number and geometry of the ED cell on the Nusselt number in ion-exchange membrane ED. An empirical correlation for the operating conditions that exist under limiting current density was proposed:

$$Nu_D = 1.793 \times \mathrm{Re}^{0.34} \times Sc^{0.329} \times (d_e / L)^{0.301} \tag{2.3}$$

where d_e is the equivalent diameter of the channel.

Sonin and Probstein [14] developed a model of the ED system to be governed by four basic similarity parameters:

1. a dimensionless applied potential.
2. the ratio of the brine and dialysate inlet concentrations.
3. a parameter measuring membrane resistance.
4. the product of channel aspect ratio and the inverse Peclet number.

They suggested an empirical equation for the estimation of total current, under a wide range of operating conditions as:

$$\hat{I} = [1 - \exp(-\hat{\psi}^3)]^{1/3} \tag{2.4}$$

where, $\hat{I}$ and $\hat{\psi}$ are dimensionless current and potential, respectively, embodying the four similarity parameters.

Shaposhnik et al. [15] developed a model for ED and suggested a simple relation to calculate average dimensionless concentration at the outlet of the ED compartment.

$$\overline{C} = 1 \pm \overline{i}l(\overline{t}_+ + \overline{t}_- - 1)/(c_0 HF\overline{v}) \tag{2.5}$$

where, $\overline{C}$ is dimensionless concentration at the outlet, $\overline{i}$ is the average current density, l is the channel length, $\overline{t}_+$ and $\overline{t}_-$ is effective transport number of the cation and anion in the membrane respectively, c_0 is inlet salt concentration, H is channel width, F is Faraday constant and $\overline{v}$ is the average velocity.

Solan and Winograd [16] worked on the boundary layer analysis of polarization in ED. For the purpose, they developed a physical model, and solved through a similarity solution. Two extreme cases were considered:

1. the undisturbed laminar flow with purely diffusive mixing.
2. the perfectly mixed flow.

In first of these, consideration of asymptotic behavior showed that a similarity solution was a relevant approximation for large values of the voltage for a large portion of the effective length of the cell. According to their results, boundary layer problem could be approximated by the similarity solution.

Lee et al. [17] studied the lactic acid recovery by ED and developed a model in which time changes in the feed and permeate volume and the electrical resistance were considered. The concentration changes with time can be represented as:

$$C = \frac{C_0 V_0 - \eta(I/F)Nt}{V_0 - \eta(I/F)\omega Nt} \tag{1.1}$$

where, C is concentration, C_0 is initial concentration, V_0 is the initial volume, η is the current efficiency, I is current, N is number of cell pairs, ω is water transport index and t is time.

Chapter 3

Theoretical Development

3.1 Modeling of a Common ED Stack

A common form of ED stack is shown in Fig 3.1, where membranes are arranged to form parallel channels. When an electric field is applied, cations (Na^+) pass through cation exchange membrane (CEM) and anion (Cl^-) pass through anion exchange membrane (AEM). In this way ion concentration in one channel reduces, whereas that is enriched in the adjoining channel. These two channels are known as diluate and concentrate channel, respectively. Further, referring Fig 3.1 the middle compartment with feed brine concentration c_0, because of the position of electrodes becomes diluate compartment. Whereas, right side of this compartment (also introduced with a brine solution of concentration c_0') become concentrate compartment. Thus, the estimation of profiles in the alternating multiple diluate and concentrate compartment may be carried out.

Further, in the diluate compartment there may be formation of two dilute boundary layers on the both inward surfaces of AEM $(X=0)$ and CEM $(X=1)$. Whereas, outward surfaces of membranes at these positions will have concentrated boundary layers.

For modeling purpose, a pair of diluate and concentrate channels with channel width H, inlet concentrations c_0 in diluate compartment and c_0' in concentrate

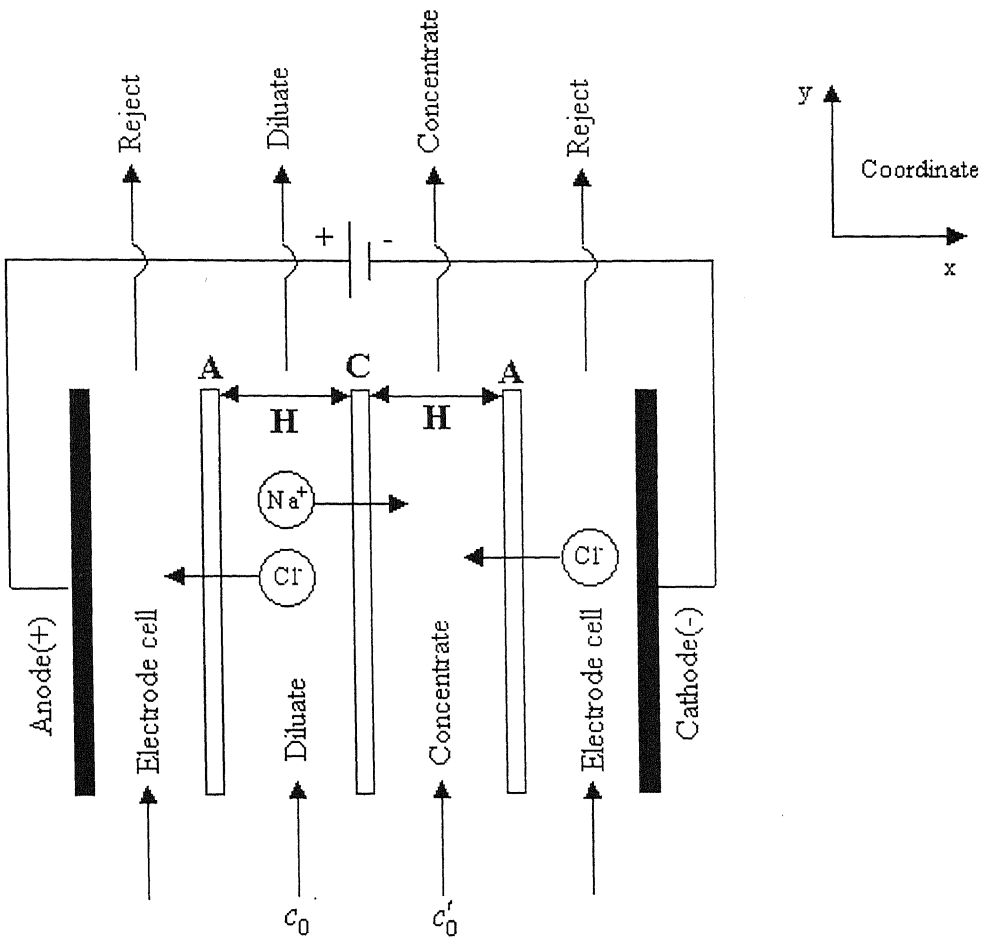

A: Anion-exchange membrane
C: Cation-exchange membrane

Fig 3.1: *Schematic of an Electrodialysis Cell Pair*

compartment, respectively, has been considered. Material balance across a differential element in a channel can be written as:

$$D\frac{\partial^2 c}{\partial x^2} = v(x)\frac{\partial c}{\partial y} \tag{3.1}$$

Here, D is diffusion coefficient, c is concentration and v is velocity in y direction. For integrating eqn. (3.1), the selected boundary conditions are:

- **For concentrate compartment:**

I. at inlet $(y=0)$, $$c = c_0 \tag{3.2}$$

II. at $x = 0$, $$-D\frac{\partial c}{\partial x} = J(y) \tag{3.3}$$

where, $J(y)$ is flux of ions at location y. The $J(y)$ may further expressed in terms of current density $i(y)$, at location y.

$$J(y) = \left(\bar{T}_+ - T_+\right)\frac{i(y)}{n_+ F} \tag{3.4}$$

Combining equations (3.3) and (3.4)

$$D\frac{\partial c}{\partial x} = -\left(\bar{T}_+ - T_+\right)\frac{i(y)}{n_+ F} \tag{3.5}$$

III. Similarly at $x = H$, $$D\frac{\partial c}{\partial x} = \left(\bar{T}_- - T_-\right)\frac{i(y)}{n_- F} \tag{3.6}$$

For non-dimensionalzing these equations, different parameters were chosen as the following:

$$x^* = H,\ y^* = \frac{\bar{v}H^2}{D},\ v^* = \bar{v},\ c^* = c_0,\ i^* = \frac{FDc_0}{H},\ \phi^* = \frac{RT}{F}$$

Non dimensional form of the equations (3.1), (3.2), (3.5) and (3.6) are as follows:

$$\frac{\partial^2 C}{\partial X^2} = V(X)\frac{\partial C}{\partial Y} \tag{3.7}$$

$$Y = 0, C = 1 \tag{3.8}$$

$$X = 0, \frac{\partial C}{\partial X} = -\left(\bar{T}_+ - T_+\right) I(Y) \tag{3.9}$$

$$X = 1, \frac{\partial C}{\partial X} = \left(\bar{T}_- - T_-\right) I(Y) \tag{3.10}$$

A similar set of equations may also be written for the diluate channel. In order to solve above set of equations, i.e. from (3.7) to (3.10), a velocity profile of the form Poiseuille distribution may be chosen [15].

$$V(X) = 6X(1-X) \tag{3.11}$$

Further, the non-dimensional current density $I(Y)$ may be estimated through a potential balance across the ED cell. The potential balance was obtained in the form of equation (3.14), by using equations (3.12) and (3.13) which are the basic definitions of ionic flux and the ionic mobility [1], respectively.

$$J_k = u_k c_k \left(-\nabla\phi\right)\frac{z_k}{n_k} \tag{3.12}$$

$$u_k = \frac{D_k n_k F}{RT} \tag{3.13}$$

$$\Delta\Phi = T_+ T_- \left(\frac{1}{z_+} - \frac{1}{z_-}\right) I(Y) \times \left[\bar{R} + \int_0^1 \frac{dX}{C(X,Y)} + \int_0^1 \frac{dX}{C'(X,Y)}\right] \tag{3.14}$$

Here Φ is dimensionless electric potential, C and C' indicate dimensionless concentration in diluate and concentrate compartment, respectively. Further, $\bar{R}$ is a relation for electrical resistance of membrane, which is given as:

$$\bar{R} = \left(\frac{d_{ma}}{\kappa_{ma}} + \frac{d_{mc}}{\kappa_{mc}} \right) \frac{\kappa_0}{H} \tag{3.15}$$

$$\kappa_0 = \left(z_+ D_+ - z_- D_- \right) \frac{F^2 c_0}{RT} \tag{3.16}$$

Where d_{ma} and d_{mc} are the thicknesses of anion and cation exchange membranes, respectively. Whereas, κ_{ma} and κ_{mc} are the conductivity of the anionic and cationic exchange membranes, respectively. κ_0 is the solution conductivity at the inlet.

Therefore, in order to obtain concentration profiles in the concentrate and diluate compartments or channels, primarily equation (3.7) was integrated numerically taking equations (3.8) to (3.16) in to account. The solutions were obtained using finite difference and Euler's technique. Details have been provided in appendix 'B'.

3.2 Prediction of Rate of Removal

In Fig 3.2, a scheme has been drawn for the prediction of rate of removal. The scheme represents a batch process where a liquid feed of sucrose solution containing calcium ion passes through the middle compartment (diluate compartment) of the ED cell. In this diluate compartment, the feed looses some of its calcium ion (Ca^{++}) by virtue of their migration to the catholyte compartment. Thus, a diluted feed, which comes of the middle compartment, is again recycled back to the same compartment

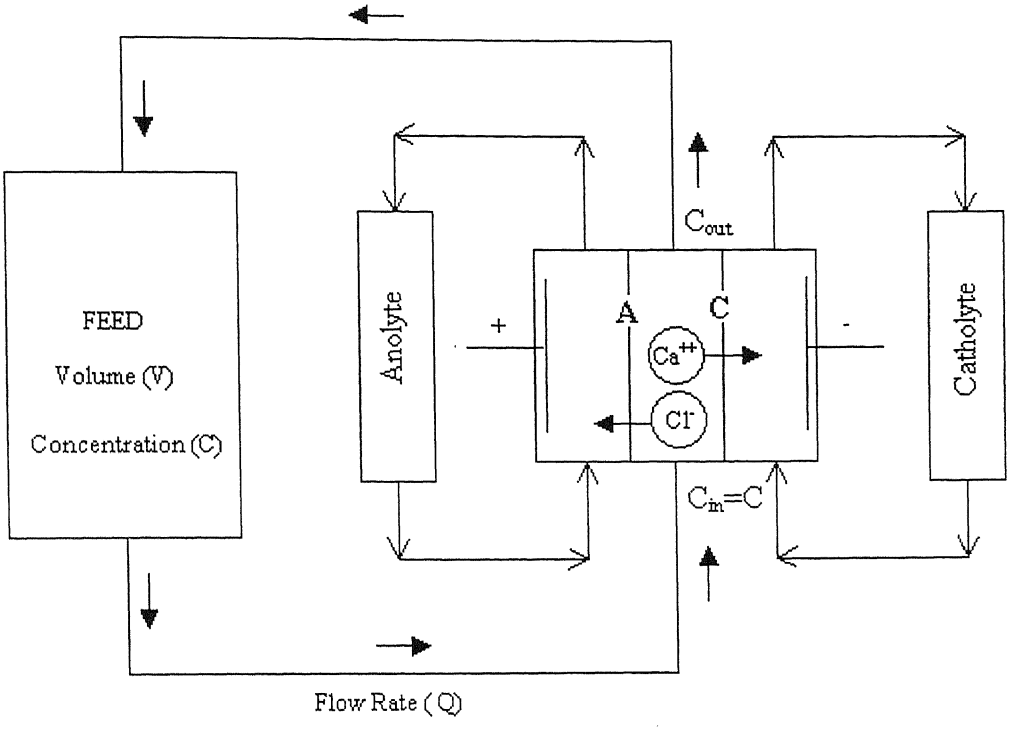

Fig 3.2: *Schematic for Rate of Removal Calculation*

via a feed tank. The process therefore, produces a feed tank solution of varying concentration of calcium ion as a function of period of ED. Material balance across the feed tank may then be obtained in terms of differential eqn. (3.17), as:

$$V\frac{dC}{dt}=Q\left(C_{out}-C\right) \tag{3.17}$$

Two types of method have been adopted in the present work for the solution of eqn. (3.17). In the first method, it was assumed that a small volume $Q\Delta t$ with concentration C comes out of the feed tank in a small time Δt as it enters into the diluate compartment. Average outlet concentration of this small volume $\left(Q\Delta t\right)$ can be estimated numerically by using the developed model in section 3.1. Therefore, this small volume $\left(Q\Delta t\right)$ with estimated concentration C_{out} is recycled back to the feed tank. It is assumed that the mixing of this volume into the feed tank is instantaneously. Therefore, new concentration C then can be calculated by material balance. Repeating such a calculation for the values of C will predict the change of concentration of the feed solution with respect to time can be calculated and so accordingly the rate of removal of calcium ion.

In the other method an analytical solution has been obtained. For dialysate compartment material balance equation in dimensionless form can be written as:

$$\frac{\partial^2 C}{\partial X^2}=V\left(X\right)\frac{\partial C}{\partial Y} \tag{3.18}$$

$$Y=0, C=1 \tag{3.19}$$

$$X=0, \frac{\partial C}{\partial X}=\left(\bar{T}_{-}-T_{-}\right)I\left(Y\right) \tag{3.20}$$

$$X=1, \frac{\partial C}{\partial X}=-\left(\bar{T}_{+}-T_{+}\right)I\left(Y\right) \tag{3.21}$$

It was assumed that there may not be significant variation in velocity across the channel width because of small channel width $\left(H \simeq 10^{-3} m\right)$ and hence $V(X)=1$. Accordingly, equation (3.18) was integrated with the applied boundary conditions stated as per equations (3.19) to (3.21) as:

$$\frac{\partial}{\partial Y}\int_0^1 C(X,Y)dX = -\left(\bar{T}_+ + \bar{T}_- - 1\right)I(Y) \tag{3.22}$$

Further, from equation (3.14), $I(Y)$ may expressed as:

$$I(Y) = \frac{K\Delta\Phi}{\left(\bar{R}_e + \int_0^1 \frac{dX}{C(X,Y)}\right)} \tag{3.23}$$

Here, $K = \left(T_+ T_- \left(\frac{1}{z_+} - \frac{1}{z_-}\right)\right)^{-1}$ which includes constants of equation (3.14);

whereas, $\bar{R}_e$ which includes resistance of membrane as well as the resistance of other compartments.

Now for further simplification of equations (3.22) and (3.23) it was assumed that there was insignificant variation in concentration across channel width, i.e. $C(X,Y)=C(Y)$. Accordingly, combining equations (3.22) and (3.23)

$$\frac{dC(Y)}{dY} = -\left(\bar{T}_+ + \bar{T}_- - 1\right)\frac{K\Delta\Phi}{\left(\bar{R}_e + \frac{1}{C(Y)}\right)} \tag{3.24}$$

Integrating eqn. (3.24)

$$\bar{R}_e\left(C_{out} - C_{in}\right) + \ln\left(\frac{C_{out}}{C_{in}}\right) = -\left(\bar{T}_+ + \bar{T}_- - 1\right)K\Delta\Phi Y \tag{3.25}$$

Further, by rearrangement $\left(\frac{C_{out}}{C_{in}}\right)$ can be written as $\left(1-\frac{C_{in}-C_{out}}{C_{in}}\right)$. For a real ED cell, for a single pass $\frac{C_{in}-C_{out}}{C_{in}} \ll 1$. Therefore, $\ln\left(\frac{C_{out}}{C_{in}}\right)$ can be approximated as $\frac{-\left(C_{in}-C_{out}\right)}{C_{in}}$. Now rearranging eqn. (3.25),

$$C_{out}-C_{in}=\frac{-\left(\bar{T}_{+}+\bar{T}_{-}-1\right)K\Delta\Phi Y}{\left(\bar{R}_{e}+\frac{1}{C_{in}}\right)} \tag{3.26}$$

Combining eqns. (3.17) and (3.26),

$$\left(\bar{R}_{e}+\frac{1}{C_{in}}\right)dC=-\left(\bar{T}_{+}+\bar{T}_{-}-1\right)K\Delta\Phi Y\frac{Q}{V}dt \tag{3.27}$$

Finally, integrating equation (3.27)

$$\bar{R}_{e}\left(C_{t}-C_{0}\right)+\ln\left(\frac{C_{t}}{C_{0}}\right)=-\left(\bar{T}_{+}+\bar{T}_{-}-1\right)K\Delta\Phi Y\frac{Q}{V}t \tag{3.28}$$

The parameter called fractional removal f_R may then be described as:

$$f_R=1-\frac{C_t}{C_0} \tag{3.29}$$

The concentration in the feed tank after a time (t) can be estimated by solving the equation (3.28) iteratively. Newton Raphson technique was used for the solution procedure. Details of solution strategy are provided in the Appendix 'B'.

Therefore, equation (3.28) will provide the rate of removal of calcium ion (Ca^{++}) from an aqueous solution of sucrose.

Chapter 4

Results and Discussions

A design problem based on boundary layers for ED with ion-exchange membranes was formulated and its analytical solutions were obtained. Therefore, through analytical approach, concentration profiles were obtained. Estimations were carried out using brine as feed in the middle compartment, as shown in Fig. 3.1. Thus, a mathematical model was developed to obtain not only concentration profiles in concentrate and diluate compartments, also it was an objective to estimate current density distribution along the flow coordinates. For convenience, all parameters were non-dimensionalized and results are presented in dimensionless form. The data used for estimations of various results and solutions are provided in appendix 'C'; whereas the coding for the solution has been included in appendix 'D'.

4.1 Concentration Profiles

A boundary layer is formed on the membrane surface when an electric current passes through an ion-exchange membrane, immersed in an aqueous solution of electrolyte. The concentration of electrolyte in the boundary layer on the separating surface falls while that on the receiving surface rises. Such a situation develops into two different types of concentration profiles in two adjacent compartments.

The main result of the modeling, therefore, is to estimate a plane concentration profile, $C = C(X,Y)$. In Fig. 4.1, concentration profiles in such two adjacent compartments (concentrate and diluate) are shown, using the developed mathematical

model, as explained in section 3.1. Further, in Fig. 4.2 and Fig. 4.3, concentration profiles in diluate and concentrate channels for different Y (direction of flow) are also presented. It may be further explained that position Y with a negligible value of 1×10^{-5} has been taken to represent the inlet condition.

It is observed from Fig. 4.2 and 4.3 that the obtained concentration profiles in these two compartments are found to behave in the obvious manner, as already described in a schematic representation of ED process in Fig. 3.1. However, in diluate compartment, it may be observed that there is less depletion at the inward surface $(X=0)$ of the AEM; whereas, there is much higher depletion of electrolyte at the inward surface $(X=1)$ of the CEM. This is because of the fact that permeation transport number of anions $(\bar{T}_- - T_- = 0.65 - 0.60 = 0.05)$ is smaller than the permeation transport number of cations $(\bar{T}_+ - T_+ = 0.70 - 0.40 = 0.30)$. In general, selectivity of the AEM is smaller than the selectivity of the CEM; hence, was chosen also accordingly [3]. Under very low concentration at the surface, the conditions at the inward surface of CEM may become severe. The situation may lead to change in pH, water splitting and their migration to different compartments, enormous power consumption, etc. However, if it is not that much severe, diffusion of ions from bulk to boundary layer may play a role to reduce the concentration difference. The above stated severe effects are more pronounced as the estimation of the concentrations are done at higher value of Y, that is the profiles away from the inlet conditions.

In concentrate compartment as shown in Fig 4.3, concentration increases in the similar fashion. These concentration profiles is calculated assuming that electrical driving force is dominating and all other effects like pressure and temperature gradients were considered to be negligible.

4.2 Current Density Distribution

As introduced in section 2.4, at the diluate side under unfavorable condition, concentration reduces such a low level that there are no further ions available for current transport. To avoid such a situation, the ED process must be operated below the limiting current density [11].

It is clear from the Fig. 4.2 that as Y increases concentration on the diluate side of the membrane goes down and particularly at $X = 1$. This reduction in the concentration results in increase in electrical resistance. Therefore, for a constant voltage, reduction in current density was observed. As soon as concentration reaches to a negligible value, condition for limiting current density is obtained. Therefore, it may be concluded that a value greater than $Y = 0.05$, may not be suitable for ED stack designed as per the other chosen variable.

With the help of the eqn. (3.14), it is possible to obtain the current density distribution along the solution flow coordinate. Fig. 4.4 shows the variation of the current density along the direction of flow. As channel length increases there is an exponential decrease of current density. The reduction of current density along the flow direction reduces the flux of the ions through membrane. Therefore, it reaches to an exponential plateau. For different potential drop, current density is different in the initial phase but it converges later. This shows that limiting current density is independent of the potential drop during higher channel length where electrical resistance of the solution dominates. This confirms the law of limiting current density as stated in equation (2.1), where it is independent of voltage. The above calculations were done for estimating the current density when potential drop was assumed to have constant value for the different Y.

4.3 Effect of Flow rate on Average Outlet Concentration

The effect Of ED process may be directly observed through the measurement of the average outlet concentration. However, average X direction concentration at each Y may be of interest in ED design, which has been already discussed in section 4.1. Fig 4.5 shows such average concentration of diluate compartment for different channel lengths at different inlet velocities. The concentration profile at that Y location was obtained and was integrated over channel width to estimate the average concentration as per:

$$\bar{C}(Y) = \frac{\int_0^1 C(X,Y)\,dX}{\int_0^1 dX} \tag{4.1}$$

It is clear that for higher flow rates, separation is much less than for lower flow rates. This is because at higher flow rates the residence time of the feed in the ED cell is smaller. The Fig 4.5 also shows that with increasing channel length the average concentration reduces, particularly during lower flow rates. For higher flow rates this drop is almost linear. These trends may help to observe an optimum channel length with respect to average concentration, which would eventually dictate the outlet concentration.

4.4 Fractional Removal of Electrolyte Solute

Fractional removal, f_R has been defined in equation (3.29) where a feed with fixed solute concentration when subjected to an ED process, gets continuously depleted. The record of change of concentration enables the calculation of f_R. It may

be mentioned that Fig 4.5 depicts average concentration at each Y for single pass of feed solution. If this diluate (outlet flow) is recycled back to the same compartment as feed; then continuous depletion will take place. However, it is clear from Fig 4.5, that the concentration change $(C_{in} - C_{out})$ in a small ED cell is not significant for a single pass. Therefore, it was intended to study these effects in a cyclic process as described in section 3.2, as well. With the help of the developed model in the final form of equation (3.28), it was possible to estimate the change in concentration with respect to time keeping other conditions fixed. Fig 4.6 was drawn to depict such a trend of fractional removal against time for different potential drops. It is clear from the figure that initially fractional removal increases linearly and later attains plateau, particularly for higher voltage. This is because at the later periods since there is drop in concentration of solute, that increases resistance, as a result of which current density reduces. This rise in fractional removal therefore becomes insignificant at later periods.

4.5 Case Study

4.5.1 Removal of Calcium Compound from Aqueous Sucrose Solution

One of the main objectives of the present work was to evaluate the developed model, using experimental results of a simple separation scheme. For the purpose, an earlier experimental investigation [5] carried out at IIT Kanpur was taken. The results of which were compared with the theoretical results predicted from the model. It was observed that the theoretical results were over-predictive than the experimental values, in general, hence not shown explicitly. This may be due to various factors;

including experimental error, choice of variables and properties, chosen for model prediction, etc. Pore blocking or membrane fouling, which reduces the efficiency of the process, may have also played a role for such non-predictive estimations.

A synthetic sucrose solution was used for experimental purpose [5]. Sucrose is a non-electrolyte, so it does not participate in the current conduction. But as time passes this sucrose may concentrate on the membrane surface, which may pose the problem for separation. Turbulence however helps in removal of any extra layer on membrane surface. In spite of this situation, a quasi-equilibrium is assumed to be attained for this continuous unsteady process. It was also observed that when current reached an asymptotic value, washing of the membrane helped to restore the current.

To deal with this problem, efficiency factor, η was introduced into the earlier developed model. This efficiency factor, η was chosen as an exponential decay factor due to the above-mentioned behaviour of sucrose precipitation, incluiding other factors as well.

$$\eta = A + (1 - A)e^{-\left(\frac{t}{\tau}\right)} \tag{4.2}$$

Introducing, η in equation (3.27)

$$\left(\bar{R}_e + \frac{1}{C_{in}}\right)dC = -\left(\bar{T}_+ + \bar{T}_- - 1\right)K\Delta\Phi\frac{Q}{V}\left(A + (1 - A)e^{-\left(\frac{t}{\tau}\right)}\right)Ydt \tag{4.3}$$

Now integrating this equation (4.3)

$$\begin{aligned}\bar{R}_e\left(C_t - C_0\right) + \ln\left(\frac{C_t}{C_0}\right) = \\ -\left(\bar{T}_+ + \bar{T}_- - 1\right)K\Delta\Phi\frac{Q}{V}\left(At - (1 - A)\tau e^{-\left(\frac{t}{\tau}\right)}\right)Y\end{aligned} \tag{4.4}$$

Equation (4.4) can be solved iteratively. For solving this equation Newton-Raphson technique was used, whereas, by trial value for A was chosen as 0.6 (dimensionless) and τ was chosen equal to $500/Q$, the unit of which is time. As the number 500 represents the volume (ml) recycled in the time τ.

4.5.2 Effect of Voltage on Rate of Removal

Fig 4.7, 4.8 and 4.9 show the effect of voltage on fractional removal at three different feed concentrations, respectively. It is evident from the figures that there is a significant increase in removal by increasing the voltage. This is due to higher driving force provided by increased voltage. It can be observed from the figures that for lower voltages $(\phi = 4 and 8V)$, the experimental results are in good agreement with predictive results. While, in case of higher voltage $(\phi = 12V)$ there is little deviation. A possible reason may be that at higher voltage the condition of limiting current density is violated, as a result of which other phenomena like water dissociation etc occurs. Due to these effects, the rate of removal may be affected and the efficiency of the actual process is reduced. Further, theoretical estimation of fractional removal was done with the assumption that the process runs much below the limiting current density.

4.5.3 Effect of Catholyte Stream Concentration on Rate of Removal

It was observed during experimental investigations [5] that membrane surface at the down streamside was getting fouled because of the deposition of the Ca^{++}. The inefficient desorption of Ca^{++} from the CEM outward surface to bulk of the catholyte solution was addressed with introduction of EDTA in the catholyte stream which

facilitating the desorption by solublizing (complex formation) the Ca^{++}. Therefore, the effect of EDTA concentration was also studied. Rate of removal was then found to increas with increase in the catholyte (EDTA) concentration as shown in Fig 4.10. Further, catholyte concentration in terms of higher ionic concentration (once EDTA dissociates in ions) may effect the fractional removal. The developed model takes in to account the concentration in catholyte compartment. Therefore, this possibility may have also increased the fractional removal.

Theoretical results were found to be in good agreement at lower catholyte (EDTA) concentrations. But in case of higher EDTA concentration, there is little deviation. This may be because of higher dosages of EDTA that might have stopped the fouling of the membrane completely. Therefore, the net efficiency would have been higher, while in theoretical development efficiency was taken constant for each case.

4.5.4 Effect of Calcium (Ca^{++}) concentration in Feed on Rate of Removal

Fig 4.11 shows the removal as a function of operating time for different Ca^{++} ion concentration. It is clear from the figure that increase in feed Ca^{++} concentration lowers the percent removal. It can be due to increased number of ions in the solution, which causes more polarization. Thus the movement of ions are slowed down.

At lower concentrations of the calcium ion, the theoretical results are not consistent with experimental results. This may be because fouling of the membranes is a function of the ion concentration. At higher concentration fouling is higher than the fouling at lower concentration. In case of theoretical estimation, this type of behaviour has not been considered, which may be a reason for inconsistency.

4.5.5 Effect of Feed Flow Rate on Rate of Removal

Fig 4.12 shows the effect of feed flow rate on the removal. Experimental results show that by increasing the feed flow rate, the rate of removal is slightly increased. However, it was also observed that further increase in feed flow rate, did not cause any significant increase in the rate of removal.

Theoretical model does not show significant change in removal by varying the feed flow rate. However, it is clear from the Fig 4.5 that for higher feed flow rate, average concentration at the outlet of the diluate cell is lower. But due to cyclic process at higher flow rates, the total volume of the feed tank is also recycled quickly. Therefore, the effect nullifies.

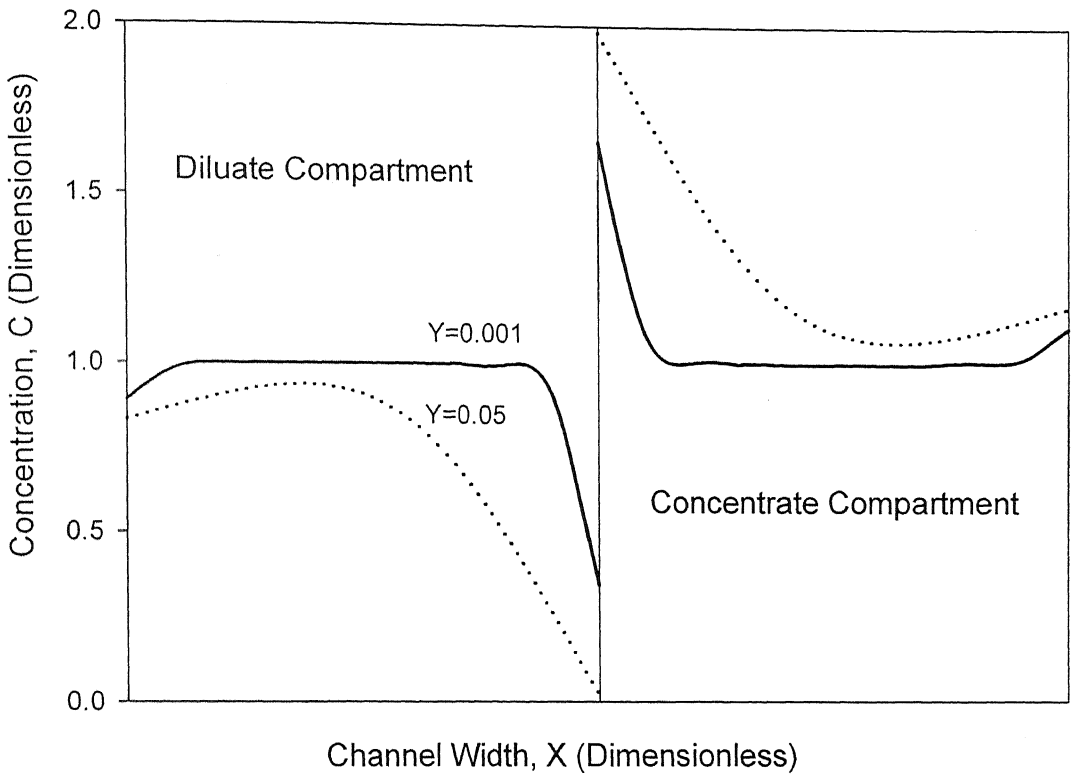

Fig 4.1: *Concentration Profiles In two Adjacent Compartments*

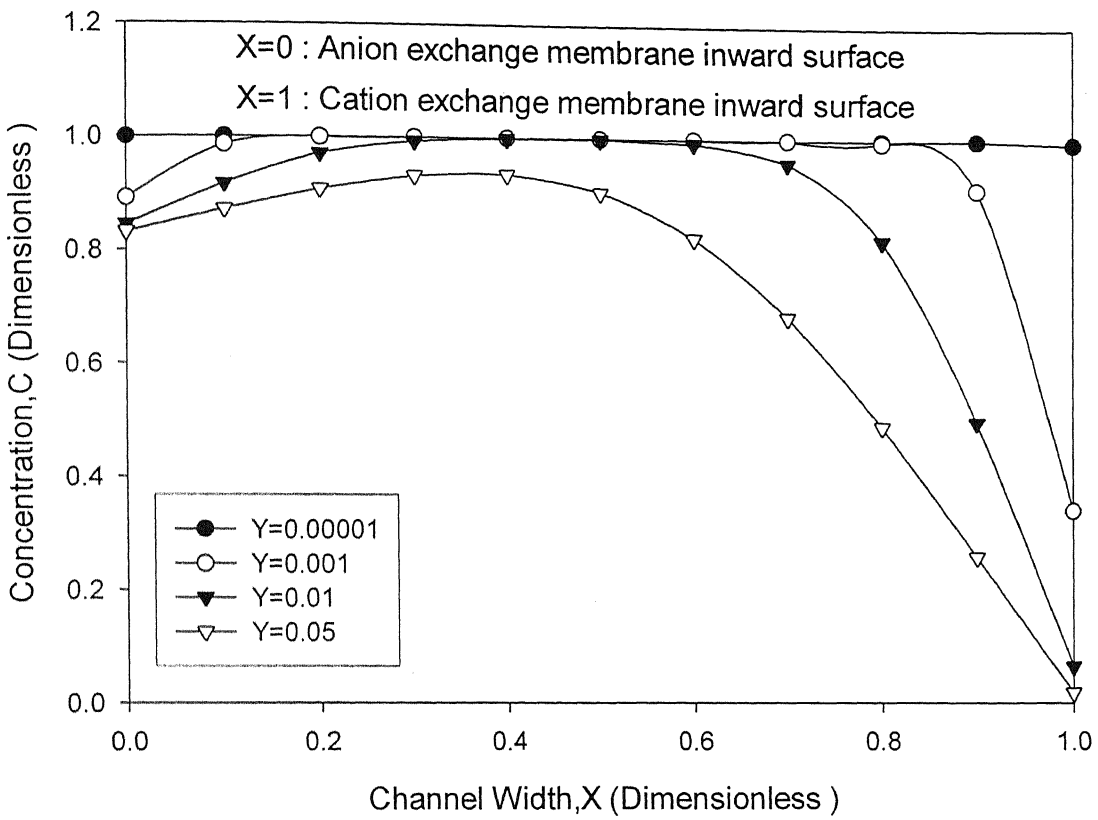

Fig 4.2: *Concentration Profiles In Diluate Compartment*

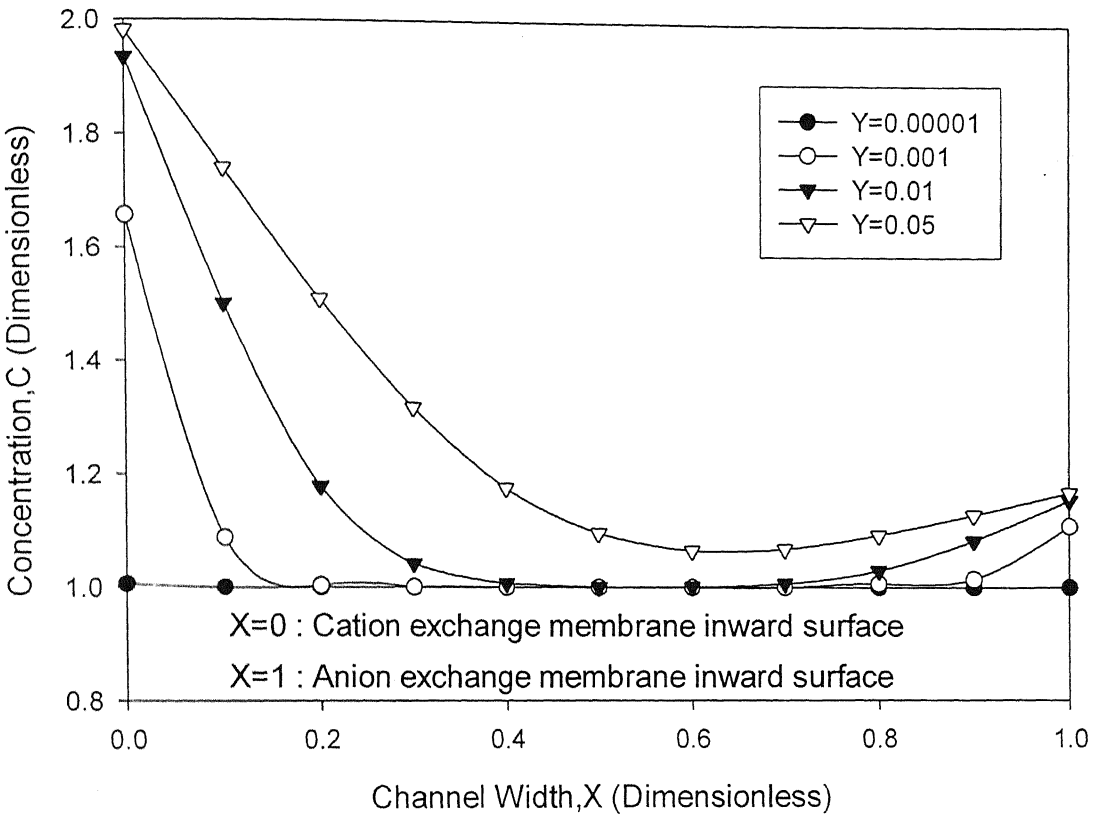

Fig 4.3: *Concentration Profiles in Concentrate Compartment*

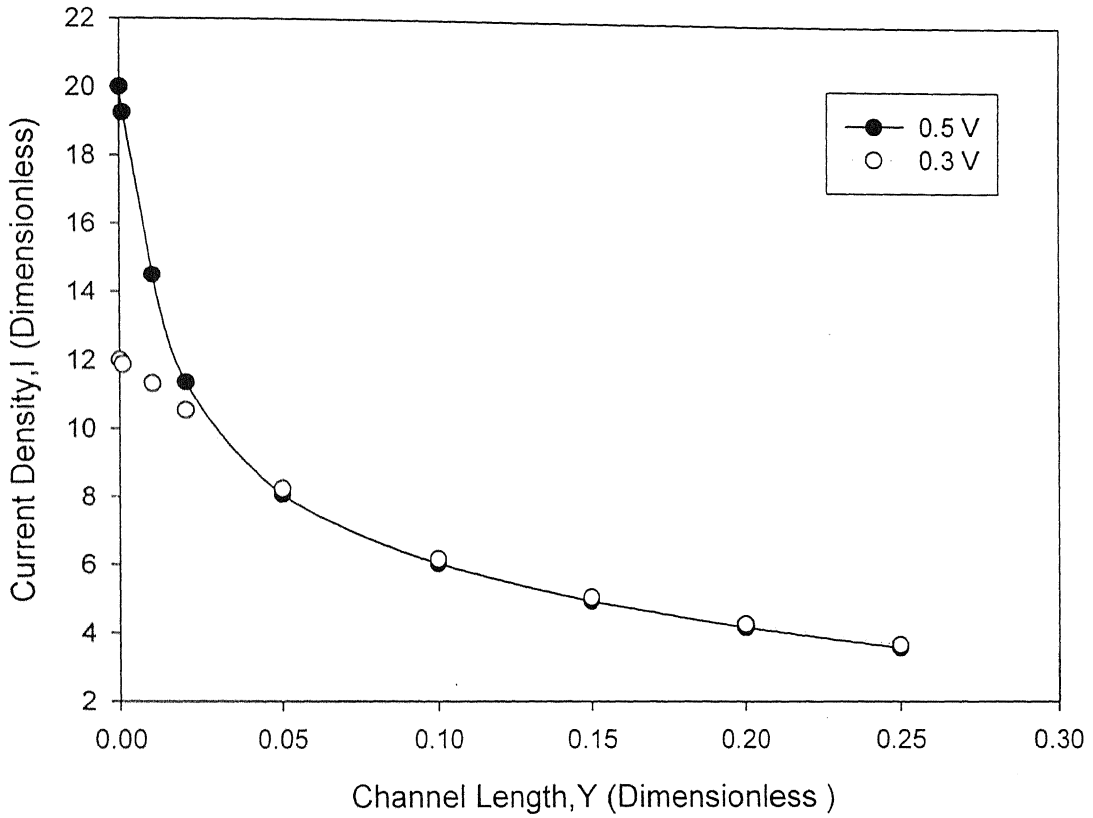

Fig 4.4: *Current Density Distribution along the Channel Length*

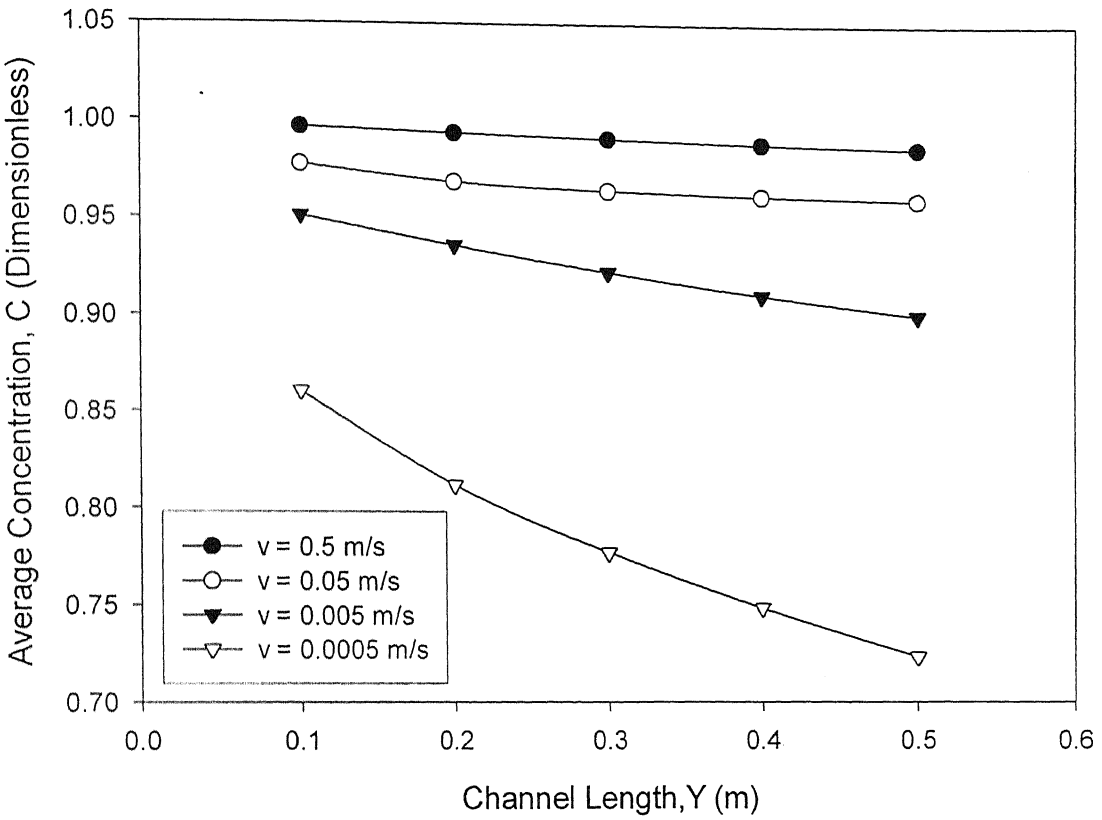

Fig 4.5: *Effect of Average Velocity on Average Outlet Concentration in Dialysate Compartment*

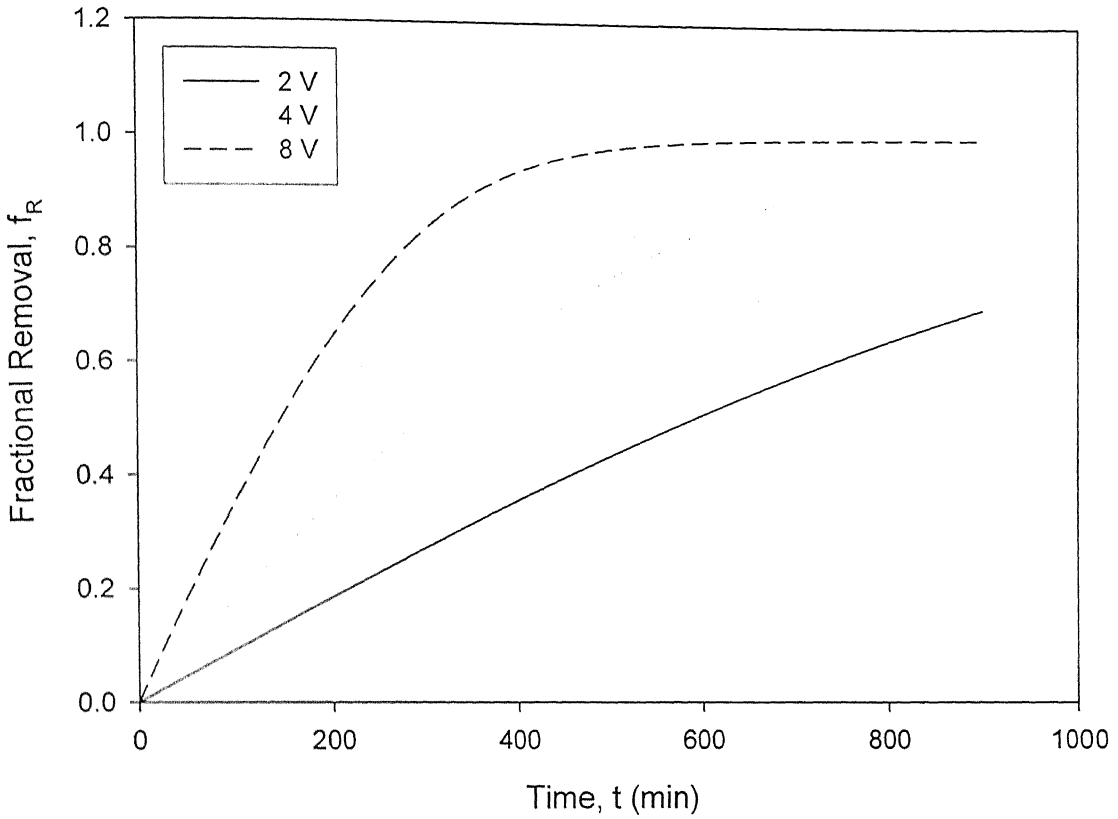

Fig 4.6:*Effect of Voltage on Rate of Removal*

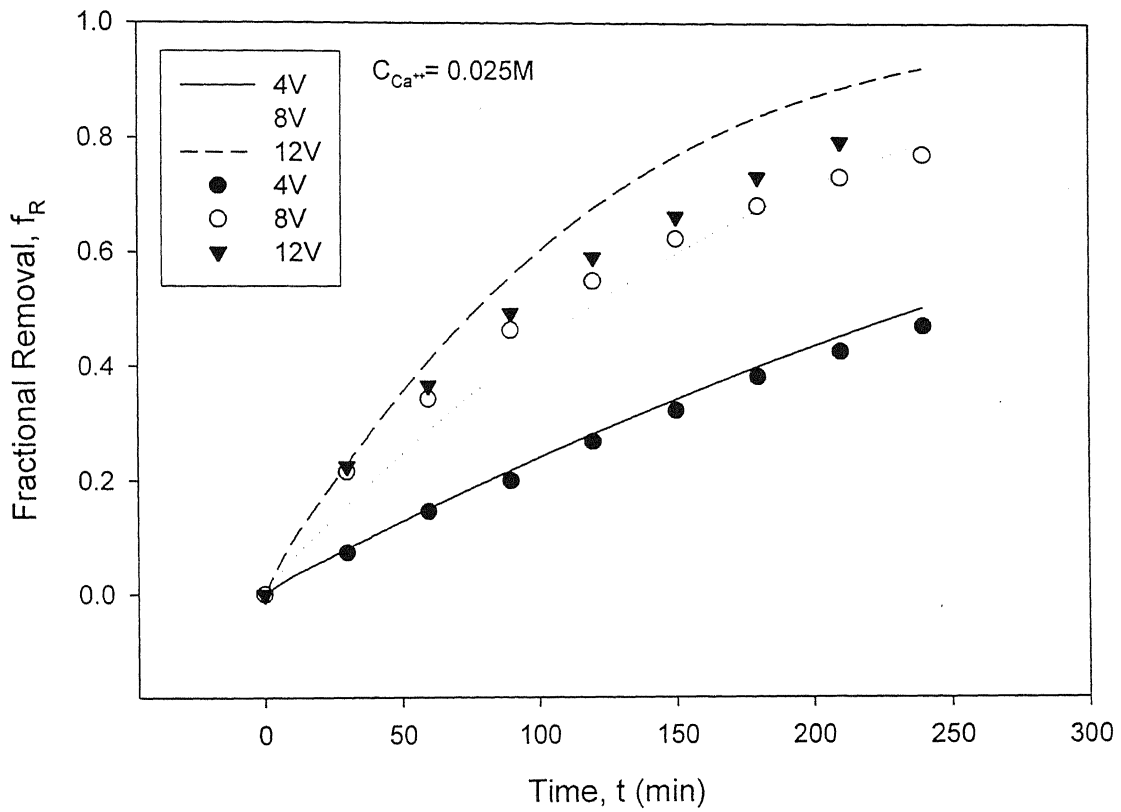

Fig 4.7: *Effect of Voltage on Rate Of Removal*

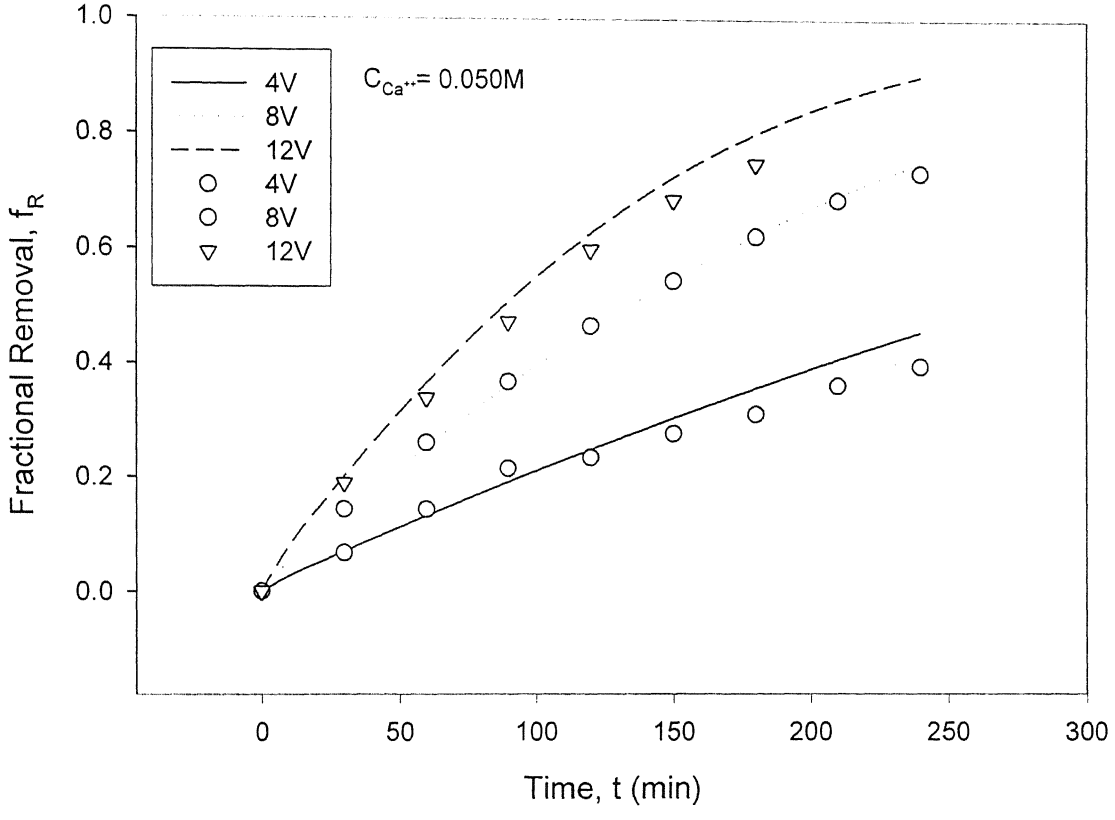

Fig 4.8: *Effect of Voltage on Rate of Removal*

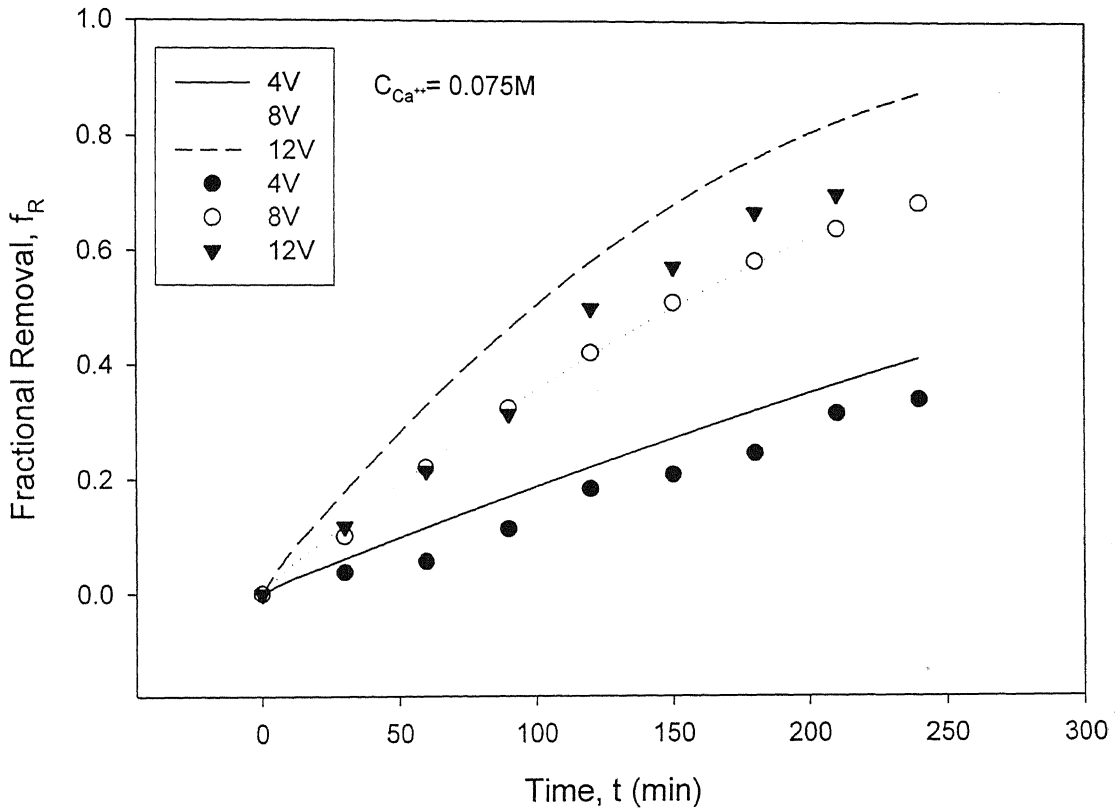

Fig 4.9: *Effect of Voltage on Rate of Removal*

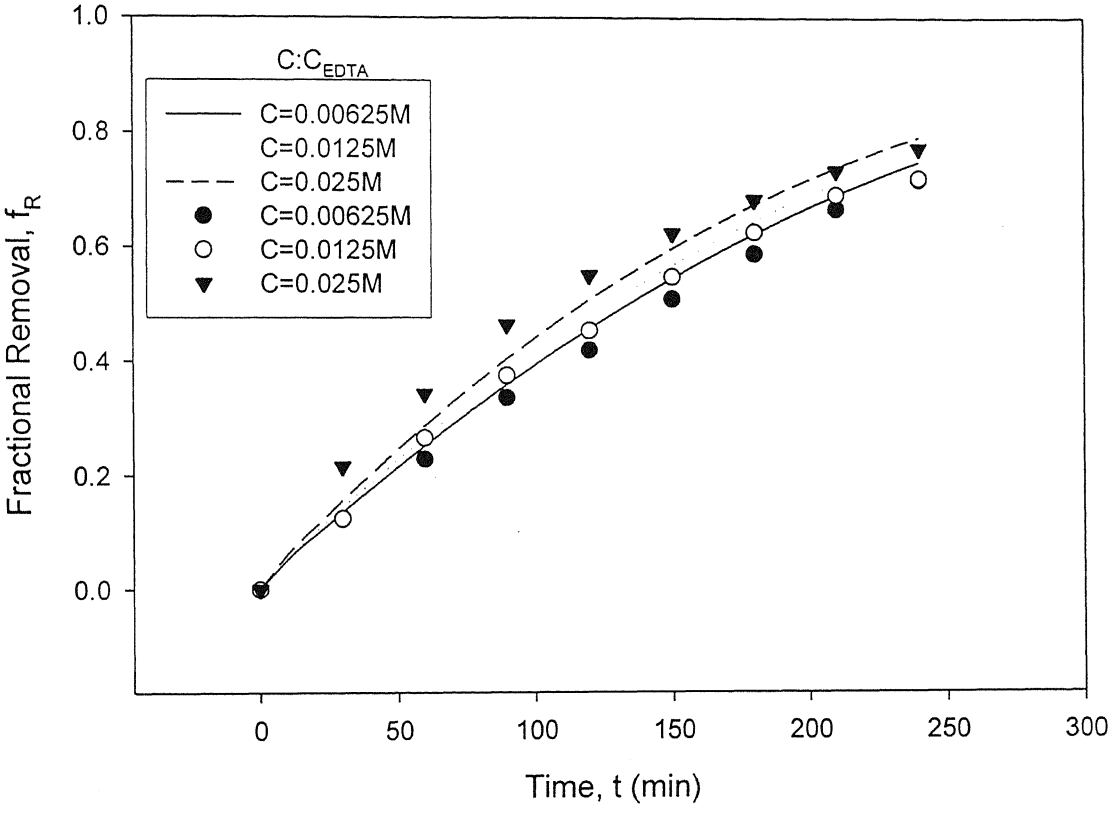

Fig 4.10: *Effect of Catholyte (EDTA) Stream Concentration on Rate of Removal*

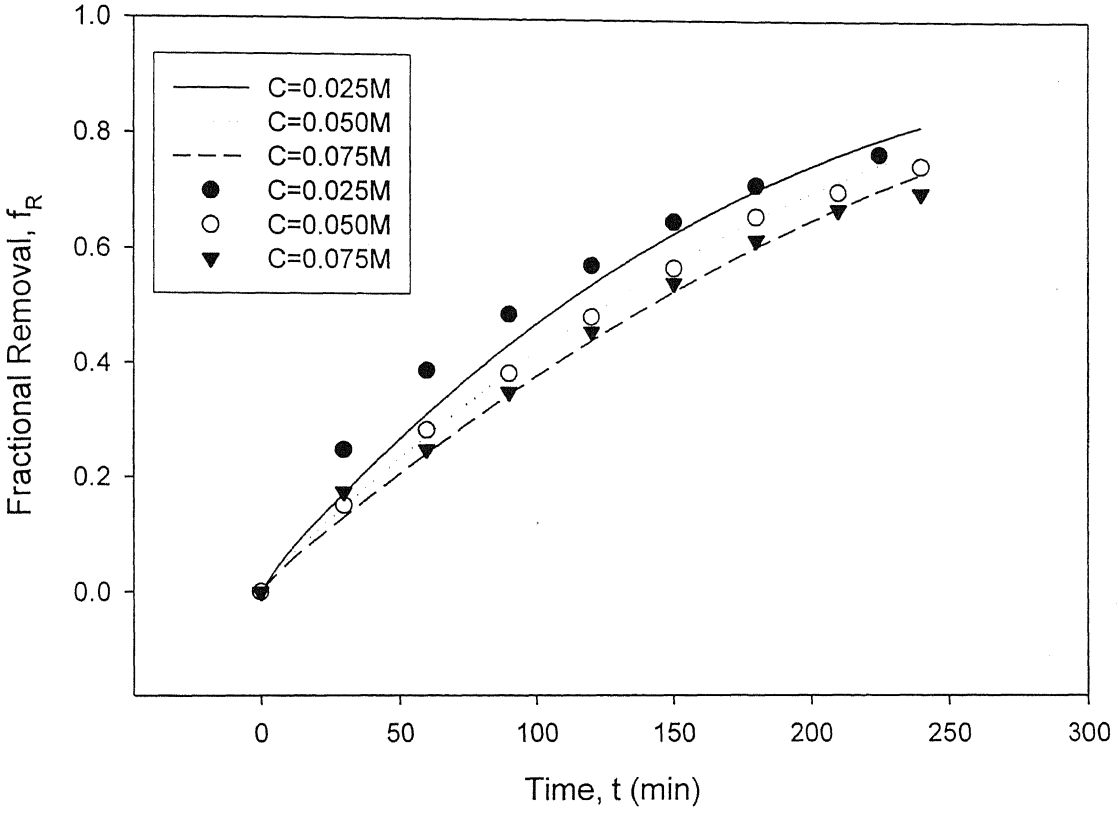

Fig 4.11: *Effect of Calcium Concentration in Feed on Rate of Removal*

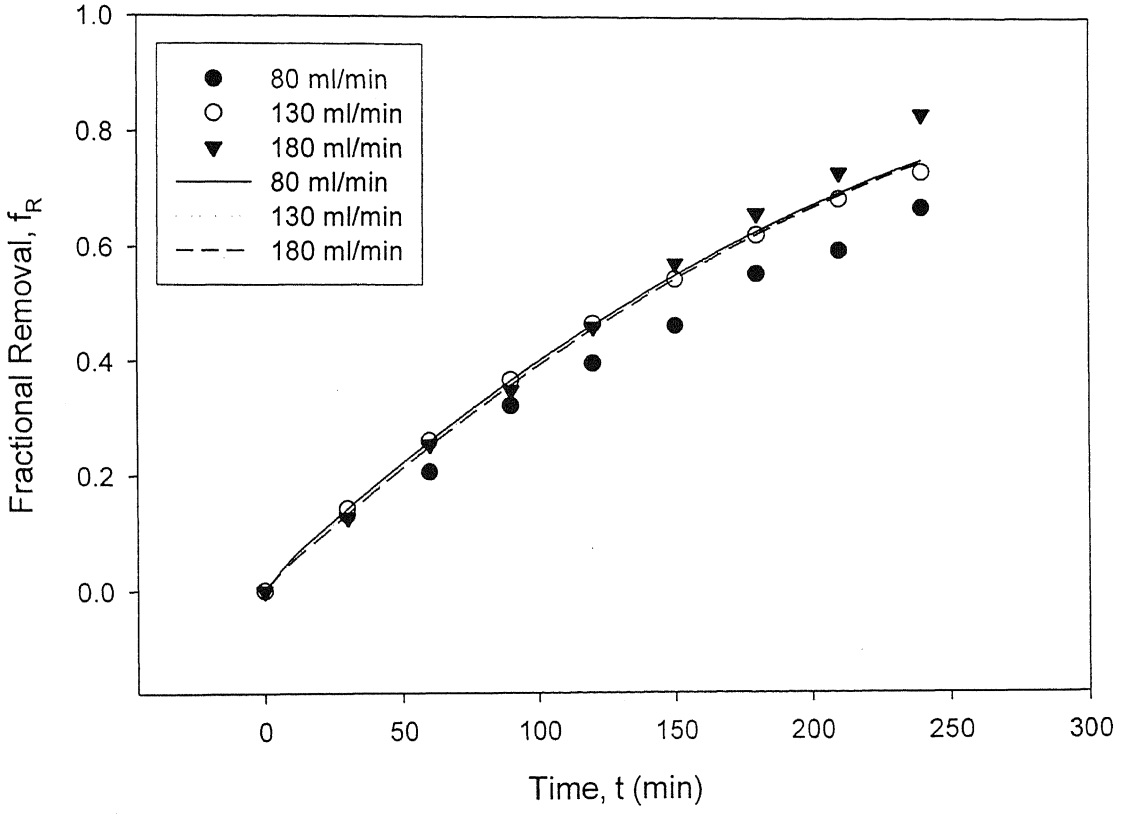

Fig 4.12: *Effect of Feed Flowrate on Rate of Removal*

Chapter 5

Conclusions and Recommendations

The theoretical modeling of a common ED stack as well as the case study has given encouraging results. However, there are some limitations of the model, which leaves a wide scope for understanding the physical process and making suitable modifications. The following conclusions are drawn from the theoretical modeling as well as from the case study:

1. As the resistance is appeared to be the function of inverse of the concentration, therefore during ED, the major electrical resistance is offered by the diluate compartment.
2. It is observed that current density reduces exponentially with the increasing channel length, therefore while designing an ED process the parameters must be chosen in such a manner that the limiting current density condition may not be violated.
3. In an ED cell, the removal is higher for relatively smaller flow rates due to higher residence time of the feed inside the cell.
4. Rate of removal increases with increase in voltage. But further increase may violate the limiting current density condition; therefore an optimum voltage must be chosen.
5. Comparison of theoretical results with experimental results shows that there are parameters like EDTA concentration that may also effect the process significantly.

Recommendations:

1. The model can be modified for various other types of ED processes with different arrangements of ion-exchange membranes or neutral membranes.
2. The efficiency factor can be further modified to include other effects like feed flow rate, feed concentration, etc.
3. It is also possible to incorporate these efficiency factors at appropriate places, while developing the model.

References

1. Shaffer, H. and Mintz, M.S., "Electrodialysis", in Spiegler, K.S. and Laird, A.D.K, (Eds.), "Principles of Desalination", Academic Press, New York, 257-357 (1980).
2. Strathman, H., "Electrodialysis and related Processes" in Noble, R.D. and Stern, S.A., (Eds.), "Membrane Separation Technology. Principles and Applications", Elsevier Science, 213-281 (1995).
3. Krol, J.J., "Monopolor and Bipolor Ion Exchange Membranes. Mass Transport Limitations", Print Partners Ipskamp, Enschede, The Netherlands (1997).
4. Sahu, A., "Modelling of Electrodialysis Process for Impurity Removal (Ca^{++} and Mg^{++}) from Sugar Cane Juice after Liming", M. Tech. Thesis, IIT Kanpur, (Dec 1994).
5. Chattopadhayay, S., "Removal of Calcium Ion from Sugar Solution through Electrodialysis", M. Tech. Thesis, IIT Kanpur, (April 1994).
6. Krol, J.J., Wessling, M. and Strathmann, H., "Concentration polarization with monopolar ion exchange membranes: current-voltage curves and water dissociation", *J. Membrane Sci.*, 162, 145-154 (1999).
7. Tanaka, Y., Iwahashi, M. and Kogure, M., "Distribution of electrodialytic condition in an electrodialyzer and limiting current density", *J. Membrane Sci.*, 92, 217-228 (1994).
8. Bobreshova, O.V. and Kulintsov, P.J., "Non equilibrium process in the concentration-polarization layers at the membrane/solution interface", *J. Membrane Sci.*, 48, 221-230 (1990).
9. Shaposhnik, V.A. and Eliseeva, T.V., "Barrier effect during the electrodialysis of ampholytes", *J. Membrane Sci.*, 161, 223-228 (1999).
10. Wen, T., Solt, G.S. and Gao D.W., "Electrical resistance and coulomb efficiency of electrodialysis (ED) apparatus in polarization", *J. Membrane Sci.*, 114, 255-262 (1996).
11. Tanaka, Y., "Concentration polarization in ion-exchange membrane electrodialysis", *J. Membrane Sci.*, 57, 217-235 (1991).

12. Cowan, D.A. and Brown, H., "Effects of turbulence on limiting current in electrodialysis cells", *Ind. Eng. Chem.*, 51, 1445-1448 (1959).
13. Huang, T. and You Yu, I., "Correlation of ionic transfer rate in electrodialysis under limiting current density condition", *J. Membrane Sci.*, 35, 193-206 (1988).
14. Sonin, A.A. and Probstein, R.F., "A hydrodynamic theory of desalination by electrodialysis", *Desalination*, 5, 293-329 (1968).
15. Shaposhnik, V.A., Kuzminykh, V.A., Grigorchuk, O.V. and Vasil'eva, V.I., "Analytical model of laminar flow electrodialysis with ion exchange membranes", *J. Membrane Sci.*, 133, 27-37 (1997).
16. Solan, A. and Winograd, Y., " Boundary-layer analysis of polarization in electrodialysis in a two-dimensional laminar flow", *The Physics of Fluids*, 12, 1372-1377 (1969).
17. Lee, E.G., Moon, S.H., Chang, Y.K., Yoo, I.K. and Chang, H.N., "Lactic acid recovery using two-stage electrodialysis and its modelling", *J. Membrane Sci.*, 145, 53-66 (1998).
18. Tragardh, G. and Gekas. V., "Membrane technology in the sugar industry", *Desalination*, 69, 9-17 (1988).

Appendix A

A.1 Experimental Details

As shown in Fig. A.1, an experimental work [5] using a three-compartment cell was taken up for case study. These compartments were Feed, Anolyte and Catholyte. All the streams were recycled back to the respective vessels. Initial volumes of the all the streams were 1000 ml.

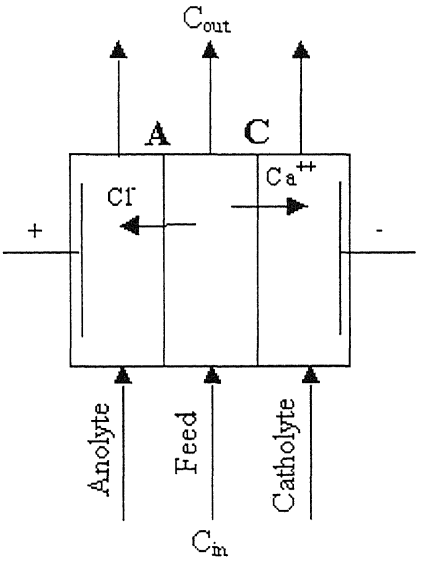

Fig A.1: *The ED Shell Used for Experimental Purpose*

Feed was taken as synthetic solutions of 5% sucrose and different concentrations of Calcium chloride ($CaCl_2$) in distilled water. Concentration of sucrose was kept constant for the all-experimental runs. Anolyte was taken as dilute solution (0.1M) of hydrochloric acid (HCl). Catholyte was taken as dilue solution of acetic acid and Ethylene diamine tetraacetic acid disodium salt (EDTA). EDTA was

added in catholyte solution to avoid the deposition of foulant layer on the CEM surface.

A.2 Data for Various Runs

Table 1: Effect of Catholyte (EDTA) Concentration on Fractional Removal

Time (min)	Fractional Removal (f_R)		
	C_{EDTA}= 0.00625M	C_{EDTA}= 0.0125M	C_{EDTA}= 0.025M
0	0.0000	0.0000	0.0000
30	0.1240	0.1250	0.2160
60	0.2290	0.2660	0.3430
90	0.3360	0.3750	0.4630
120	0.4190	0.4530	0.5490
150	0.5080	0.5470	0.6234
180	0.5870	0.6250	0.6816
210	0.6650	0.6900	0.7323
240	0.7160	0.7190	0.7715

Voltage: 8 volt
Feed flow rate: 130 ml/min
Anolyte flow rate: 830 ml/min
Catholyte flow rate: 830 ml/min
Feed Concentration: 0.025M
Anolyte Concentration: 0.100M
Catholyte Concentration: EDTA: C_{EDTA}
AA: 0.025M

Table 2: Effect of Calcium ion (Ca^{++}) Concentration in Feed on Fractional Removal

Time (min)	Fractional Removal (f_R)		
	C_{Ca}=0.025M	C_{Ca}=0.050M	C_{Ca}=0.075M
0	0.0000	0.0000	0.0000
30	0.2480	0.1509	0.1740
60	0.3876	0.2831	0.2484
90	0.4870	0.3828	0.3496
120	0.5720	0.4822	0.4562
150	0.6490	0.5678	0.5417
180	0.7123	0.6577	0.6173
210		0.7002	0.6704
225	0.7670		
240		0.7455	0.6995

Voltage: 8 volt
Feed flow rate: 130 ml/min
Anolyte flow rate: 830 ml/min
Catholyte flow rate: 830 ml/min
Feed Concentration: C_{Ca}
Anolyte Concentration: 0.100M
Catholyte Concentration: EDTA: 1* C_{Ca}
AA: 2*C_{Ca}

Table 3: Effect of Feed Flow Rate (Q) on Fractional Removal

Time (min)	Fractional Removal (f_R)		
	Q: 80ml/min	**Q: 130ml/min**	**Q: 180ml/min**
0	0.0000	0.0000	0.0000
30	0.1322	0.1432	0.1270
60	0.2066	0.2605	0.2540
90	0.3223	0.3671	0.3490
120	0.3967	0.4653	0.4600
150	0.4628	0.5439	0.5711
180	0.5537	0.6220	0.6590
210	0.5950	0.6850	0.7300
240	0.6694	0.7323	0.8316

Voltage: 8 volt
Anolyte flow rate: 830 ml/min
Catholyte flow rate: 830 ml/min
Feed Concentration: 0.050M
Anolyte Concentration: 0.100M
Catholyte Concentration: EDTA: 0.050M
AA: 0.050M

Table 4: Effect of Voltage $\Delta\varphi$ on Fractional Removal

Time (min)	Fractional Removal (f_R)								
	Run 1			Run 2			Run 3		
	Feed Concentration : 0.025M Anolyte Concentration : 0.100M Catholyte Concentration : EDTA : 0.025M AA : 0.025 M			Feed Concentration : 0.050M Anolyte Concentration : 0.100M Catholyte Concentration : EDTA : 0.050M AA : 0.050 M			Feed Concentration : 0.075M Anolyte Concentration : 0.100M Catholyte Concentration : EDTA : 0.075M AA : 0.075 M		
	$\Delta\varphi$ =4 V	$\Delta\varphi$ =8 V	$\Delta\varphi$ =12 V	$\Delta\varphi$ =4 V	$\Delta\varphi$ =8 V	$\Delta\varphi$ =12 V	$\Delta\varphi$ =4 V	$\Delta\varphi$ =8 V	$\Delta\varphi$ =12 V
0	0.0000	0.0000	0.0000	0.0000	0.0000	0.0000	0.0000	0.0000	0.0000
30	0.0730	0.2160	0.2250	0.0670	0.1432	0.1889	0.0380	0.1010	0.1180
60	0.1454	0.3430	0.3660	0.1430	0.2605	0.3386	0.0570	0.2210	0.2150
90	0.1997	0.4630	0.4930	0.2150	0.3671	0.4724	0.1140	0.3246	0.3140
120	0.2685	0.5490	0.5910	0.2350	0.4653	0.5984	0.1835	0.4218	0.4990
150	0.3230	0.6234	0.6620	0.2770	0.5439	0.6850	0.2090	0.5100	0.5720
180	0.3820	0.6816	0.7319	0.3110	0.6220	0.7480	0.2470	0.5831	0.6680
210	0.4265	0.7323	0.7942	0.3613	0.6850		0.3164	0.6400	0.7000
240	0.4709	0.7715		0.3950	0.7323		0.3407	0.6852	

Feed flow rate: 130 ml/min, Anolyte flow rate: 830 ml/min, Catholyte flow rate: 830 ml/min

Appendix B

B.1 Solution Strategy

$$\frac{\partial^2 C}{\partial X^2} = V(X)\frac{\partial C}{\partial Y} \tag{B.1}$$

For solving equation (B.1) Finite Difference and Euler's technique has been used. For this domain $(0 \le X \le 1)$ has been divided in to $N+1$ equispaced grid points. e.g. a 6 points grid has been shown in the Fig B.1.

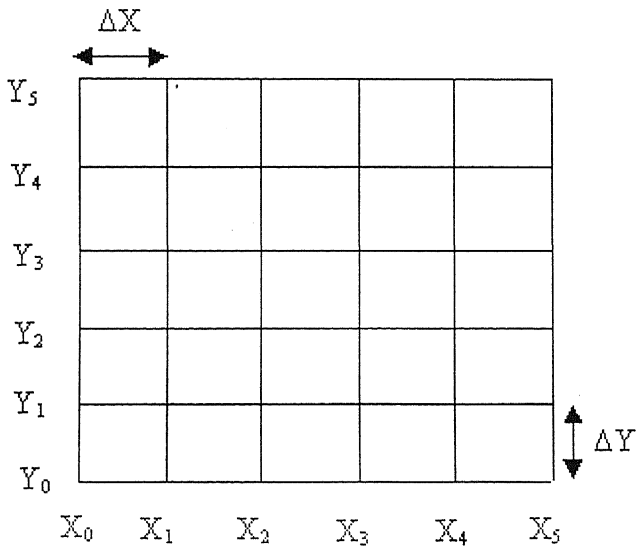

Fig B.1: *The Grid Points Used in Finite Difference and Euler's Technique*

Now, expressions for $\frac{dC}{dX}$ and $\frac{d^2C}{dX^2}$ at location (X_i, Y_k) can be written as:

$$\frac{dC_i^k}{dX} = \frac{C_i^k - C_{i-1}^k}{\Delta X} \tag{B.2}$$

$$\frac{d^2C_i^k}{dX^2} = \frac{C_{i+1}^k - 2C_i^k + C_{i-1}^k}{(\Delta X)^2} \tag{B.3}$$

For calculating $\frac{dC}{dX}$ and $\frac{d^2C}{dX^2}$ at boundary grid points, The value of C at two imaginary grid points (X_{-1}, X_{N+1}) should be known. This can be taken care by boundary conditions, where the value of $\frac{dC}{dX}$ is known. So the value of C at imaginary grid points can be estimated. Therefore, $\frac{d^2C}{dX^2}$ can be calculated at boundary points.

Now replacing these values of $\frac{d^2C}{dX^2}$ at location (X_i, Y_k) in equation (B.1), the values of $\frac{dC}{dY}$ at location (X_i, Y_k) can be calculated. For further estimation of C values at location (X_i, Y_{k+1}) Euler's technique has been used.

$$C_i^{k+1} = C_i^k + \Delta Y \times \frac{dC_i^k}{dY} \tag{B.4}$$

This way the values of C can be calculated at different grid points. For calculation of $I(Y)$ in equation (3.14), the integral $\int_0^1 \frac{dX}{C(X,Y)}$ needs to be calculated. This is calculated using trapezoidal method.

For following the above given procedure a code in C has been written, which has been attached in the appendix C.

For solving equation (3.28) Newton Raphson technique was used. The equation (3.28) can be written in form of eqn. (B.5)

$$F(C) = 0 \tag{B.5}$$

Solution can be achieved iteratively by eqn. (B.6)

$$C^{k+1} = C^{k} - \frac{F(C)}{F'(C)} \tag{B.6}$$

where F' denotes the derivative of the function. For this a code in C has been written, which has been attached in the appendix C.

Appendix C

Data Used for Estimation of Concentration Profile

- Channel width, H = 2.0 mm
- Diffusion coefficient, D = 2*10^{-6} cm^2/sec
- Faraday constant, F = 96500 amp-sec/equivalent
- Feed concentration, $c_0 = c_0'$ = 0.01M
- $\bar{T}_+$ = 0.90, $\bar{T}_-$ =0.65
- T_+ = 0.40, T_- =0.60
- $d_{ma} = d_{mc}$ = 0.1 mm
- $\kappa_{ma} = \kappa_{mc}$ = 0.1 ohm^{-1} m^{-1}

Data Used for Case Study

- Channel Length, y = 8.8 mm
- Membrane Surface Area = 8.8 * 4.2 Cm^2
- $\bar{T}_+$ = 0.91, $\bar{T}_-$ =0.90
- T_+ = 0.44, T_- =0.56

Rest of the data other than feed concentration was same as used for concentration profile predictions. The feed concentrations were chosen according to experimental conditions.

Appendix D

- **Code for Estimating Concentration Profiles**

```
#include"temp.h"

/*************************************************************************
 * BY INCLUDING TEMP.H OTHER NECESSARY FILES AND REQUIRED INPUT HAS     *
 * BEEN TAKEN. C AND C1 IS USED FOR DILUATE AND CONCENTRATE COMPARTMENT*
 * RESPECTIVELY.                                                        *
 * FUNCTION main() FIRST INITIALIZES THE CONCENTRATIONS.                *
 * THEN IT ITERATIVELY USES FUNCTION FIN_DIFF() AND EULER() TO GET      *
 * THE UPDATED VALUE AT NEXT Y POSITION AND SIMULTANEOUSLY THESE VALUES*
 * ARE WRITEN TO OUTPUT FILES.                                          *
 *************************************************************************/


int main(void)
 {
  FILE *ofp1,*ofp2,*ofp3;
  float C[SIZE],y[SIZE],C1[SIZE],y1[SIZE];
  int i,j;


for(i=0;i<SIZE;i+=1)
   {
    C[i]=1;
    C1[i]=1;
   }
  ofp1=fopen("outfile1","w");
  ofp2=fopen("outfile2","w");
  ofp3=fopen("outfile3","w");
  for(i=0;i<SIZE;i+=1)
   {
    fprintf(ofp1,"%7.4f\t ",x[i]);
    fprintf(ofp2,"%7.4f\t ",x1[i]);
   }
    fprintf(ofp1,"\n");
    fprintf(ofp2,"\n");
  for(j=0;j<N;j++)
    {
     if(j%10==0)

fprintf(ofp3,"%7.4f\t%7.4f\t%7.4f\n",CURRENT(C,C1),AVERAGE(C),AVERAGE(C1))
;
     FIN_DIFFf(C,y,C1,y1);
     EULER(C,y,C1,y1);
     if(j%10==0)
```

```
    {
     for(i=0;i<SIZE;i+=1)
       {
        fprintf(ofp1,"%7.4f\t ",C[i]);
        fprintf(ofp2,"%7.4f\t ",C1[i]);
       }
        fprintf(ofp1,"\n");
        fprintf(ofp2,"\n");
    }
    }
  fclose(ofp1);
  fclose(ofp2);
  fclose(ofp3);
  return 0;
 }

/*****************************************************************
 * FUNCTION FIN_DIFF() USES FINITE DIFFERENCE TECNIQUE AS       *
 * STATED IN EQUATION B.3 (APPENDIX B) AND PROVIDES THE         *
 * REQUIRED GRADIENTS                                           *
 *****************************************************************/

void FIN_DIFF(float *p,float *q,float *r,float *s)
 {
  int i;
  float v,a,b,cur;
  cur=current(p,r);
  a=0.05*cur;
  b=-0.3*cur;
  for(i=0;i<SIZE;i++)
    {
     if(i==0)
      {
       q[i]=(p[i+1]-p[i]-a*H)/(H*H*0.01);
       s[i]=(r[i+1]-r[i]-b*H)/(H*H*0.01);
      }
     else if(i==(SIZE-1))
      {
       q[i]=(p[i-1]-p[i]+b*H)/(H*H*0.01);
       s[i]=(r[i-1]-r[i]+a*H)/(H*H*0.01);
      }
     else
      {
       v=6*i*H*(1-i*H);
       q[i]=(p[i+1]-2*p[i]+p[i-1])/(H*H*v);
       s[i]=(r[i+1]-2*r[i]+r[i-1])/(H*H*v);
      }
    }
 }

/*****************************************************************
 * FUNCTION EULER() UPDATES THE VALUE OF CONCENTRATION AS       *
 * DESCRIBED IN EQUATION B.4 (APPENDIX B).                      *
 *****************************************************************/

void EULER(float *p,float *q,float *r,float *s)
```

```
 {
  int i;
  for(i=0;i<SIZE;i++)
   {
    p[i]=p[i]+K*q[i];
    r[i]=r[i]+K*s[i];
   }
 }


/*****************************************************************
 * FUNCTION CURRENT() TAKES THE VALUES OF CONCENTRATION IN BOTH*
 * COMPARTMENTS AT A FIXED Y AND PROVIDES CURRENT DENSITY AT    *
 * THAT LOCATION Y                                              *
 *****************************************************************/

float CURRENT(float *p,float *r)
 {
  int i;
  float curr,sum=0,sum1,resi=0.014934;
  sum=1/p[0]+1/p[SIZE-1]+1/r[0]+1/r[SIZE-1];
  for(i=1;i<SIZE-1;i++)
    sum+=2*(1/p[i]+1/r[i]);
  sum=0.5*H*sum;
  sum=sum+resi;
  curr=(V*38.69)/(sum*0.48);
  return(curr);
 }

/*****************************************************************
 * FUNCTION AVERAGE() INTEGRATES THE FUNCTION USING TRAPEZOIDAL *
 * METHOD                                                       *
 *****************************************************************/

float AVERAGE(float *p)
 {
  int i;
  float sum=0;
  for(i=0;i<SIZE;i++)
   {
    sum+=2*p[i];
   }
  sum=0.5*H*(sum-p[0]-p[SIZE-1]);
  return(sum);
 }
```

File Temp.h

```
#include<stdio.h>
#include<stdlib.h>
#include<math.h>

#define SIZE 11 /* number of points in the x direction on used grid*/
#define H 0.1  /* Step size in X direction*/
#define K 1e-6 /*step sixe in Y direction*/
#define N 250000 /* Number of iterations to be carried out*/
#define V 0.5   /* Applied Voltage*/

void fin_diff(float *,float *,float *,float *);
void euler(float *,float *,float *,float *);
float current(float *,float *);
float AVERAGE(float *);
```

- **Code for Estimating Concentration Profiles**

```
#include<stdio.h>
#include<math.h>
#define TL 1e-6
#define HEIGHT 8.8
#define FRMULTI 396.8254
#define CONCNMULTI 1.4934

/*****************************************************************
 * THIS PROGRAM TAKES INPUT FROM A FILE. FIRST ALL PARAMETER ARE*
 * CALCULATED ACCORDINGLY. AND THEN NEWTON RAPHSON TECHNIQUE HAS*
 * BEEN USED TO CALCULATE THE CONCENTRATION AT PARTICULAR TIME  *
 * AND THAT HAS BEEN STORED IN A OUTPUT FILE.                   *
 *****************************************************************/

int main(void)
 {
  float c,c0=1.0,c1,c2,beta,RESI,FR,val,deri;
  float YRANGE,CANO,CCATH,CF,VOLT,EFC;
  int time;

  FILE *ofp1,*ofp2;

  ofp2=fopen("infile","r");
  fscanf(ofp2,"%f",&FR);
  fscanf(ofp2,"%f",&CF);
  fscanf(ofp2,"%f",&CCATH);
  fscanf(ofp2,"%f",&CANO);
  fscanf(ofp2,"%f",&VOLT);
  fscanf(ofp2,"%f",&EFC);
  printf("%f\t%f\t%f\t%f\t%f\n",FR,CF,CCATH,CANO,VOLT);
  fclose(ofp2);

  YRANGE=HEIGHT/(FRMULTI*FR);
  RESI=CF*CONCNMULTI+CF/CCATH+CF/CANO;
  printf("%f\t%f\n",RESI,YRANGE);

  /*beta=(0.81*38.69*VOLT/0.48)*(FR/1000)*YRANGE;*/
  printf("%f\n",beta);
  beta=(0.81*38.69*VOLT/0.3696)*(FR/1000)*YRANGE;

  c2=c0;
  ofp1=fopen("outfile2","w");
  for(time=10;time<=240;time+=10)
  {
   c=c2;
   do
    {
     val=RESI*(c-c0)+log(c/c0)+beta*(EFC*time+((1-EFC)*(500/FR)) //
    *(1-exp(-(FR/500)*time)));
     deri=RESI+1/c;
     c1=c-val/deri;
     if(fabs(c-c1)>TL)
       c=c1;
```

```
    else
      break;
   }while(1);
  fprintf(ofp1,"%7.5f\n",1-c1);
  c2=c1;
}
 fclose(ofp1);
 return 0;
}
```

Input file for the above code:

```
180             /*FLOW RATE IN (ml/min) */
0.05            /*FEED CONCENTRATION (M)*/
0.1             /*CATHOLYTE CONCENTRATION (M)*/
0.1             /*ANOLYTE CONCENTRATION (M)*/
8               /* APPLIED VOLTAGE (V)*/
0.6             /* A IN EFFICIENCY FACTOR */
```